



## **JGR** Oceans

#### **RESEARCH ARTICLE**

10.1029/2025JC022777

#### **Key Points:**

- Using the NFSV-assimilation, the central Pacific (CP)- and eastern Pacific (EP)-intermediate coupled climate models are constructed with the abilities of simulating CP and EP El Niño events, respectively
- Both enhancing wind forcing and thermocline effects can lead to a stronger CP El Niño, but they undergo different mechanisms
- Wind-dominated CP El Niño is driven by advective feedback whereas thermocline-dominated CP event is driven by thermocline feedback

#### **Supporting Information:**

Supporting Information may be found in the online version of this article.

#### Correspondence to:

W. Duan, duanws@lasg.iap.ac.cn

#### Citation:

Tao, L., & Duan, W. (2025). Exploration on dynamics of El Niño diversity based on nonlinear forcing singular vector-assimilation approach. *Journal of Geophysical Research: Oceans, 130*, e2025JC022777. https://doi.org/10.1029/2025JC022777

Received 22 APR 2025 Accepted 10 OCT 2025

#### **Author Contributions:**

Conceptualization: Lingjiang Tao,
Wansuo Duan
Data curation: Lingjiang Tao
Formal analysis: Lingjiang Tao
Funding acquisition: Lingjiang Tao
Investigation: Lingjiang Tao
Methodology: Lingjiang Tao
Methodology: Lingjiang Tao
Resources: Lingjiang Tao
Software: Lingjiang Tao

Supervision: Wansuo Duan
Validation: Lingjiang Tao, Wansuo Duan
Visualization: Lingjiang Tao
Writing – original draft: Lingjiang Tao
Writing – review & editing:
Lingjiang Tao, Wansuo Duan

© 2025. American Geophysical Union. All Rights Reserved.

# **Exploration on Dynamics of El Niño Diversity Based on Nonlinear Forcing Singular Vector-Assimilation Approach**

Lingjiang Tao<sup>1,2</sup> and Wansuo Duan<sup>3,4</sup>

<sup>1</sup>State Key Laboratory of Climate System Prediction and Risk Management, Nanjing, China, <sup>2</sup>School of Marine Sciences, Nanjing University of Information Science and Technology, Nanjing, China, <sup>3</sup>State Key Laboratory of Earth System Numerical Modeling and Application, Institute of Atmospheric Physics, Chinese Academy of Sciences, Beijing, China, <sup>4</sup>University of Chinese Academy of Sciences, Beijing, China

Abstract Climate models still encounter challenges in simulating the El Niño diversity, namely the central Pacific (CP) and eastern Pacific (EP) El Niño. This limitation restricts the climate study and prediction. The present study employs the nonlinear forcing singular vector (NFSV)-assimilation method to optimize an intermediate coupled climate model (ICM). With the NFSV-assimilation, two types of optimized forcing vectors (OFVs) corresponding to CP and EP El Niño are derived: CP-OFV and EP-OFV. These vectors representing unresolved mechanisms related to El Niño types are used to drive the ICM, thereby constructing CP-ICM and EP-ICM. The CP- and EP-ICMs can effectively characterize the evolutions and air-sea coupling processes of CP and EP El Niño, respectively. Further, based on the CP-ICM, sensitivity experiments are devised to explore the impacts of the wind forcing and thermocline on the CP El Niño simulations. Both the intensification of the wind forcing and thermocline effects warm the CP but the former tends to cool the EP from the sensitivity experiments. The distinct effect in the EP is attributed to the meridional advection. For the CP, the underlying mechanisms also vary. The CP warming is mainly attributed to the zonal advection feedback in the wind-dominated climate system whereas the thermocline feedback also serves as a crucial oceanic process in the thermocline-dominated climate system. This research not only deepens the understanding of the dynamic of the CP El Niño but also provides an effective model platform for further studying the El Niño diversity.

Plain Language Summary Both central Pacific (CP) and eastern Pacific (EP) El Niño events are important interannual variabilities driving short-term climate change. However, current models have poor skills in simulating their differences, hampering climate understanding, and prediction. To overcome the limitation, this study uses the nonlinear forcing singular vector-assimilation method to improve a simplified climate model. By assimilating the observations, we identify the unique forcing vectors that represent unresolved mechanisms in the CP and EP El Niño simulation with the model, respectively. By embedding these vectors into the model, the CP- and EP-intermediate coupled climate model (ICM) capable of simulating the two types of El Niño, respectively, are successfully constructed. These two models can not only accurately depict the distinct evolutions of the two types of El Niño but also simulate the corresponding air-sea interaction mechanisms. Furthermore, the wind forcing and thermocline effects on the CP El Niño evolutions are investigated based on the CP-ICM, revealing the distinct adjustment effects of oceanic processes on the sea surface temperature in the CP during different warming phases. This study not only reveals the dynamic mechanism of the CP El Niño but also provides an effective model tool for subsequent research on the predictability of El Niño diversity.

#### 1. Introduction

The theoretical exploration of the El Niño-Southern Oscillation (ENSO) phenomenon spans multiple decades. Improved observations and contributions from international researchers have catalyzed the formulation of diverse ENSO conceptual frameworks. These models emerged under different theoretical frameworks (Battisti, 1988; N. Chen & Majda, 2016; Fang et al., 2024a, 2024b; Jin, 1997; Latif et al., 1993; Zebiak & Cane, 1987; Zhang et al., 2003). Concurrently, advancements in high-performance computing architectures over recent decades have precipitated transformative progress in comprehensive earth system modeling. The exponential growth in computational efficiency and data storage capacities has facilitated the emergence of multinational collaborative endeavors such as the Coupled Model Intercomparison Project (see <a href="https://www.wcrp-climate.org/wgcm-cmip/wgcm-cmip6">https://www.wcrp-climate.org/wgcm-cmip/wgcm-cmip6</a>). These projects provide a solid foundation for scholars worldwide to analyze and diagnose global weather and climate changes (Tokarska et al., 2020).

TAO AND DUAN 1 of 20

Notwithstanding these advancements, simulations of ENSO complexity remain suboptimal (Timmermann et al., 2018). It is the diversity in horizontal distribution of El Niño that constitutes a pivotal facet underpinning the complexity of the ENSO phenomenon. According to the location of the warming center, the El Niño phenomena are categorized into two distinct classifications: central Pacific (CP) and eastern Pacific (EP) El Niño. For the purpose of exploring the ENSO complexity, lots of conceptual models are successfully built to model the CP and EP El Niño (e.g., N. Chen et al., 2022; T. Geng et al., 2020; Vialard et al., 2025). Whereas, relatively complex coupled models fail to capture this diversity. Although L. Geng and Jin (2023) provided a seemingly feasible way to make the intermediate coupled ocean-atmosphere model (ICM) have the ability to produce El Niño diversity in a range of nonlinearity, most conventional ICMs demonstrate capacity solely for simulating a single type of El Niño (Duan et al., 2014; Zhang et al., 2003). Yu and Kim (2010) scrutinized the performance of models from CMIP3 in simulating the El Niño diversity, revealing that even sophisticated climate models predominantly generated one type of El Niño. Moreover, CMIP3 had large biases compared to observations regarding the development and decay of both types of El Niño (Leloup et al., 2008). Even in CMIP5, the models still exhibit substantial systematic biases. For example, the interannual variability of sea surface temperature (SST) in the tropical Pacific simulated by some models is skewed westward relative to observations (Capotondi, 2013; Choi et al., 2011; Kug et al., 2010). Most models cannot accurately distinguish the meridional positions of SST anomalies related to EP and CP El Niño (Feng et al., 2020). Recently, Hou and Tang (2022) conducted a comprehensive evaluation of 19 CMIP5 models and their updated CMIP6 counterparts regarding their simulation capabilities for two types of El Niño. The analysis revealed that although CMIP6 models demonstrate marked enhancements in replicating the intensities and patterns of both El Niño types, they exhibited negligible amelioration in simulating their periodic diversity. Notably, some individual models performed even worse in periodicity simulations compared to their predecessors.

The prevailing discourse on the deficiencies in simulating El Niño diversity remains divergent. Yu and Fang (2018) posited that inadequate simulation of seasonal footprint mechanism contributions relative to recharge-discharge dynamics fundamentally constrains the simulation of ENSO diversity. They pointed out that the seasonal footprint mechanism can make ENSO more complex, whereas the recharge-discharge mechanism makes the ENSO cycle more regular. It is a weak seasonal foot mechanism and a strong recharge-discharge mechanism represented in current models that make it hard to simulate ENSO diversity. Ham and Kug (2012) attribute the inability of models to simulate different types of El Niño to the cold bias in the eastern tropical Pacific in the models. For instance, the SST biases in the equatorial Pacific contribute to a weak climatological zonal SST gradient over the western-central equatorial Pacific. This attenuated gradient consequently compromises the efficacy of the zonal advection feedback mechanism, thereby rendering the simulation of CP El Niño events less favorable within current climate modeling frameworks (Feng et al., 2020). Kim et al. (2012) argued that models exhibit limited capacity in delineating the impact of the North Pacific Oscillation on the central tropical Pacific, thus resulting in weak zonal advection feedback and producing CP El Niño weaker than in the observations. To this end, incorporating stochastic processes describing the wind bursts and interdecadal variations of the background Walker circulation and correcting the subsurface processes, N. Chen and Fang (2023) renewed the ICM to successfully reproduce the intensity, occurrence frequency, and spatial patterns of EP and CP El Niño events realistically.

The inadequacies in simulating ENSO diversity within climate models are intrinsically linked to uncertainties in comprehending the dynamics of ENSO variability. Some studies emphasize the pivotal role of local and stochastic wind (including those triggered by extratropical processes) in equatorial dynamics (Ashok et al., 2007; D. K. Chen et al., 2015; M. Y. Chen et al., 2021; Ding et al., 2017; Yang et al., 2023). Some perspectives attribute ENSO diversity to thermocline perturbations (Chung & Li, 2013; McPhaden et al., 2011; Xu et al., 2017). A prevailing scholarly inclination, however, posits that the combined effect of atmospheric forcing and thermocline dynamics drives the ENSO diversity (Fedorov et al., 2015; S. N. Hu et al., 2014; Lai et al., 2015; Zhi et al., 2019). Therefore, both wind and thermocline constitute indispensable sources of predictability in the prediction of ENSO diversity (Fang & Mu, 2018).

To advance our comprehension of ENSO diversity, substantial endeavors remain imperative in model calibration and refinement. However, given that climate models are approximations of the complex Earth system with error sources being manifold and pervasive throughout simulations, incremental improvements to individual physical processes may yield limited efficacy in modeling both CP and EP El Niño. Particularly, sources of uncertainty in ENSO diversity simulations are intricate with various physical processes exerting distinct influences on the

TAO AND DUAN 2 of 20

modeling of ENSO. Consequently, it is neither feasible nor practical to isolate or examine them individually. To solve this problem, Duan et al. (2014) attributed all model error sources to model tendency errors and proposed a new variant of the nonlinear forcing singular vector (NFSV) approach. By implementing the new version of the NFSV approach to optimize an ICM, they successfully replicated both CP and EP El Niño events observed in nature. Given that the methodological framework bears resemblance to data assimilation, it has recently been designated as NFSV-assimilation and has seen incremental application in enhancing predictive accuracy for high-impact meteorological events and climatic projections (Tao et al., 2020, 2022; Zheng et al., 2023).

In this study, the NFSV-assimilation is applied to an ICM from the Institute of Oceanology at the Chinese Academy of Sciences (Zhang & Gao, 2016). With the NFSV-related forcing vectors, two models corresponding to the two types of El Niño are constructed, which enables the ICM to accurately simulate the temporal and spatial evolution characteristics of the CP and EP El Niño. In addition, the present study will continue to explore the impacts of wind forcing and thermocline effect on the development of the CP El Niño based on the CP El Niño-related ICM, and clarify the dominant physical processes influencing the warming location of El Niño. The results of this study will contribute to the understanding of the dynamics and origins of the CP El Niño as well as the diversity of the ENSO.

Section 2 describes the design of the NFSV-assimilation approach with the ICM. Section 3 shows the constructed models related to EP and CP El Niño and evaluates their performance in El Niño simulation. Section 4 discusses the distinct impacts of the wind forcing and thermocline effects on the simulation of CP El Niño. A summary and discussion are given in Section 5.

#### 2. NFSV-Assimilation With the ICM

The ICM adopted in the present study is a highly simplified atmosphere-ocean coupled model that only represents the physics and thermodynamics in the tropical Pacific (Zhang et al., 2003). In the ICM, the air-sea coupling is concisely characterized by the relationship between SST and wind stress anomaly  $(\tau)$ , which is described as

$$\tau = \alpha_{\tau} \cdot F(SST),\tag{1}$$

where  $\alpha_{\tau}$  denotes the relative strength of wind forcing effect. The subsurface temperature ( $T_{\text{sub}}$ ) is derived via parameterization of sea level (SL) anomalies using the equation

$$T_{\text{sub}} = \alpha_T \cdot \mathbf{G}(\text{SL}),\tag{2}$$

where  $\alpha_T$  denotes the thermocline effect on the surface to some extent. Since the ICM can well characterize SST-wind interaction and thermocline feedback processes, it behaves high performance in simulating the transition between the cold and warm phases of ENSO. Nevertheless, precisely because the ICM overlooks the interactions among diverse physical processes within the complex climate system, the simulated ENSO structure is relatively regular (Zhang et al., 2008), rendering it challenging to simulate the two types of El Niño events (Tao & Duan, 2019). Considering the aforementioned advantages and limitations of the ICM, we are confident that we can further calibrate the model using the NFSV-assimilation method, thereby being capable of simulating both CP and EP El Niño events.

The NFSV-assimilation is a nontraditional assimilation approach that focuses on model errors and attempts to modify the model tendency equation through the assimilation of observations, allowing the simulated results to approximate the observed ones (Duan et al., 2014; Tao & Duan, 2019; Zheng et al., 2023). Here, we are concerned with the SST evolution related to ENSO and attribute all model uncertainties to the SST model tendency equation of the ICM. That is, the forcing vector is added into the SST model during the NFSV-assimilation analysis. Hence, the SST model with the time-dependent forcing vector ( $f_i$ ) of the ICM is mathematically described as follows:

$$\frac{\partial X}{\partial t} = M(X, t) + f_t,\tag{3}$$

where X represents the monthly SST anomaly and M(X,t) denotes the original dynamic framework of the SST model. For more detailed information about the SST model of the ICM, readers are referred to Zhang and

TAO AND DUAN 3 of 20

$$J(f_t^*) = \min \sum_{t=t_0}^{t_0 + n\Delta t} \|X(f_t, t) - X^{\text{obs}}(t)\|,$$
(4)

where  $X^{\rm obs}$  is the observed monthly SST anomaly; n denotes the length of the assimilation window;  $f_t^*$  is the optimized forcing vector (OFV) that allows the ICM-simulated SST anomalies to be closest to observations. It is worth noting that when considering the adjustments of the ocean and the atmosphere, the adjustment of the ocean is a relatively slow process, while that of the atmosphere is a relatively fast one. Thus, we hypothesize that tendency perturbation in the SST model of the ICM remains constant over a 1-month period. This treatment is consistent with previous studies (e.g., Duan et al., 2014; Tao et al., 2022). Additionally, a discussion on the time step of the tendency perturbation is presented in Text S1 in Supporting Information S1. Then, according to Equation 4, we can calculate a series of monthly NFSV-optimized forcing vectors (NOFVs). If Equation 4 approaches zero, the NOFVs characterize to a certain extent the overall effect of the missed processes in the ICM on the SST evolution. From an alternative viewpoint, the OFVs represent the physical processes that are absent or misdescribed in the ICM.

Two data sets are used to perform the NFSV-assimilation and evaluate the performance. One is the SST data from the extended reconstructed data of version fifth at NOAA (ERSSTv5; Huang et al., 2017). Another is from the Global Ocean Data Assimilation System (GODAS) reanalysis (Behringer et al., 1998). By assimilating the SST field during the period from 1960 to 2020, we finally obtain a large number of monthly NOFV samples (totally  $(2020 - 1960 + 1) \times 12 = 732$ ). When these forcing vectors are superimposed into the SST model of the ICM to simulate the SST anomaly in the tropical Pacific from 1960 to 2020, it can be found that the model can relatively accurately simulate the observed evolution of SST anomaly related to ENSO. This result further validates the efficacy of the NOFVs we derived. As in the previous studies (Tao & Duan, 2019; Tao et al., 2020), the NOFVs are flow-dependent, of which the distributions are highly correlated with the SST anomaly in the tropical Pacific. This indicates that when the ICM simulates El Niño with a specific type, it always fails to characterize a certain physical process resulting in similar tendency errors in the model tendency. Although we cannot ultimately determine which key physical process is missing or misrepresented in the model, we can obtain the model tendency errors (which actually refer to NOFVs here) when simulating El Niño with a specific type.

To extract the commonalities of model errors in simulating EP or CP El Niño, the NOFVs are initially classified into sets of NOFVs related to EP El Niño and those related to CP El Niño. For instance, when  $X^{\text{obs}}(t)$  in Equation 4 represents the SST anomalies observed during EP El Niño years, the OFVs are categorized as EP El Niño-related NOFVs sets. Subsequently, each set of forcing vectors is synthesized according to the corresponding calendar month so that seasonal NOFVs related to different types of El Niño events from January to December are obtained. The composite CP El Niño-related and EP El Niño-related NOFVs can reflect the typical characteristics of missed or misdescribed dynamics in simulating CP and EP El Niño, respectively. The former set of vectors is referred to as CP-OFV, whereas the latter set is referred to as EP-OFV.

Figure 1 displays the spatiotemporal characteristics of the obtained CP-OFV and EP-OFV. It is evident that the spatial distributions of CP-OFV and EP-OFV are different, indirectly indicating that the CP and EP El Niño events have different physical mechanisms. The EP-OFV is mainly distributed in the equatorial EP and the north-south boundaries of the model (Figure 1d). The EP-OFV shows a dipole distribution pattern along the equator with positive values in the east and negative values in the west (Figure 1e). Outside the equator, the positive forcing dominates. The former may be related to the errors that occur when the model simulates equatorial processes, whereas the latter may be associated with the missing extratropical forcing factors. From a temporal standpoint, the time-dependence of the EP-OFV is relatively weak (Figure 1f), whereas the CP-OFV is dependent on the calendar month (Figure 1c). The signal of CP-OFV in the equatorial region is mainly negative in winter and spring but turns positive in summer and autumn (Figure 1b). Furthermore, when considering the intensity of the forcing vectors, the magnitude of the CP-OFV is greater than that of the EP-OFV. This implies that, in contrast to the EP El Niño, the ICM encounters more severe challenges in simulating the CP El Niño.

TAO AND DUAN 4 of 20

21699291, 2025, 10, Downloaded from https://agupubs.onlinelibrary.wiley.com/doi/10.1029/2025JC022777 by Wansuo Duan - Institution Of Atmospheric Physics , Wiley Online Library on [21/10/2025]. See the Terms

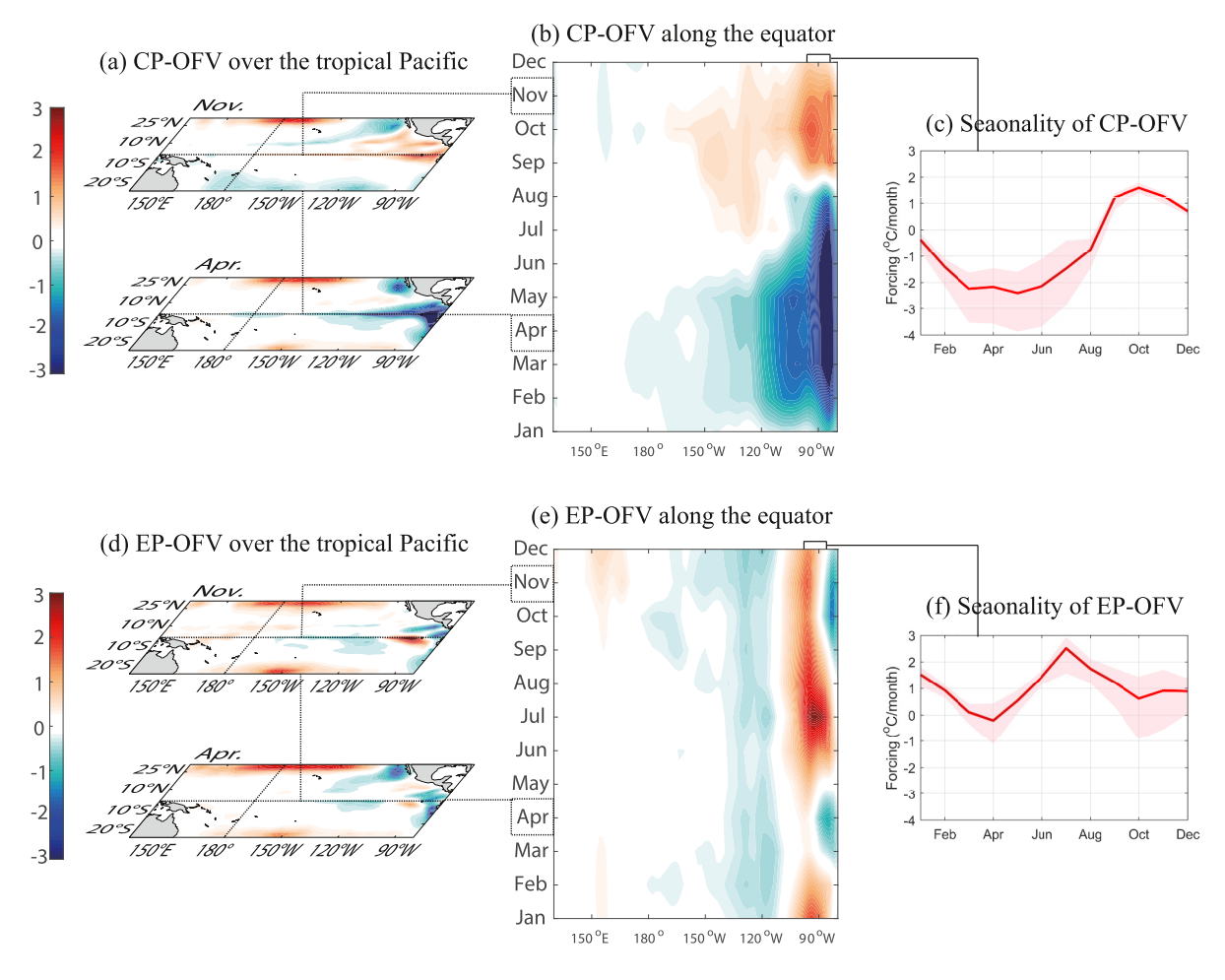


**Figure 1.** Spatiotemporal distributions of the central Pacific-optimized forcing vector (CP-OFV) and eastern Pacific (EP)-OFV (unit: °C/month) in the intermediate coupled climate model during CP and EP El Niño simulations. Panels (a) and (d) show the horizontal distribution of CP- and EP-OFV in November and April, respectively. Panels (b) and (e) are the temporal evolutions along the equator. Panels (c) and (d) denote the seasonality of CP- and EP-OFV in a certain region (5°S–5°N, 100°W–86°W).

The negative value of the CP-OFV in spring and summer indicates that the ICM has a significant warm bias in this region when simulating the CP El Niño event. Clearly, this contradicts the observations, which show that the SST anomaly during the occurrence of CP El Niño is largely suppressed in spring and summer. Previous studies have pointed out that the zonal wind anomalies of the CP El Niño in spring are more westward compared to those of the EP El Niño (Fang et al., 2024a, 2024b; Li et al., 2025). This finding indicates that the wind-induced Rossby waves are closer to the western Pacific boundary. Consequently, the time required for these wind-induced Rossby waves to transform into upwelling Kelvin waves via the Bjerknes feedback and subsequently suppress the increase in SST in the EP is shorter (Fang et al., 2024a, 2024b). Therefore, the cooling bias in the simulation of CP El Niño may be due to the fact that the position of the zonal wind stress simulated in spring is too far eastward. From this perspective, CP-OFV is likely to reflect the effect of the wind on the EP during CP El Niño.

#### 3. EP and CP El Niño-Related Models and Their Performances

As previously mentioned, distinct OFVs represent the total effects of those processes that cannot be captured during the simulation of EP or CP ENSO. When these ENSO type-related OFVs (i.e., CP-OFV and EP-OFV) are reintroduced into the ICM, they can offset the model deficiencies, thereby establishing different models capable of simulating the corresponding ENSO types. For instance, when seasonally cycling EP-OFVs are used to force the ICM, theoretically, it is expected that an EP El Niño-related model (hereafter termed EP-ICM) can be constructed. From a mathematical perspective, this essentially entails substituting the forcing vector  $f_i$  in Equation 3

TAO AND DUAN 5 of 20

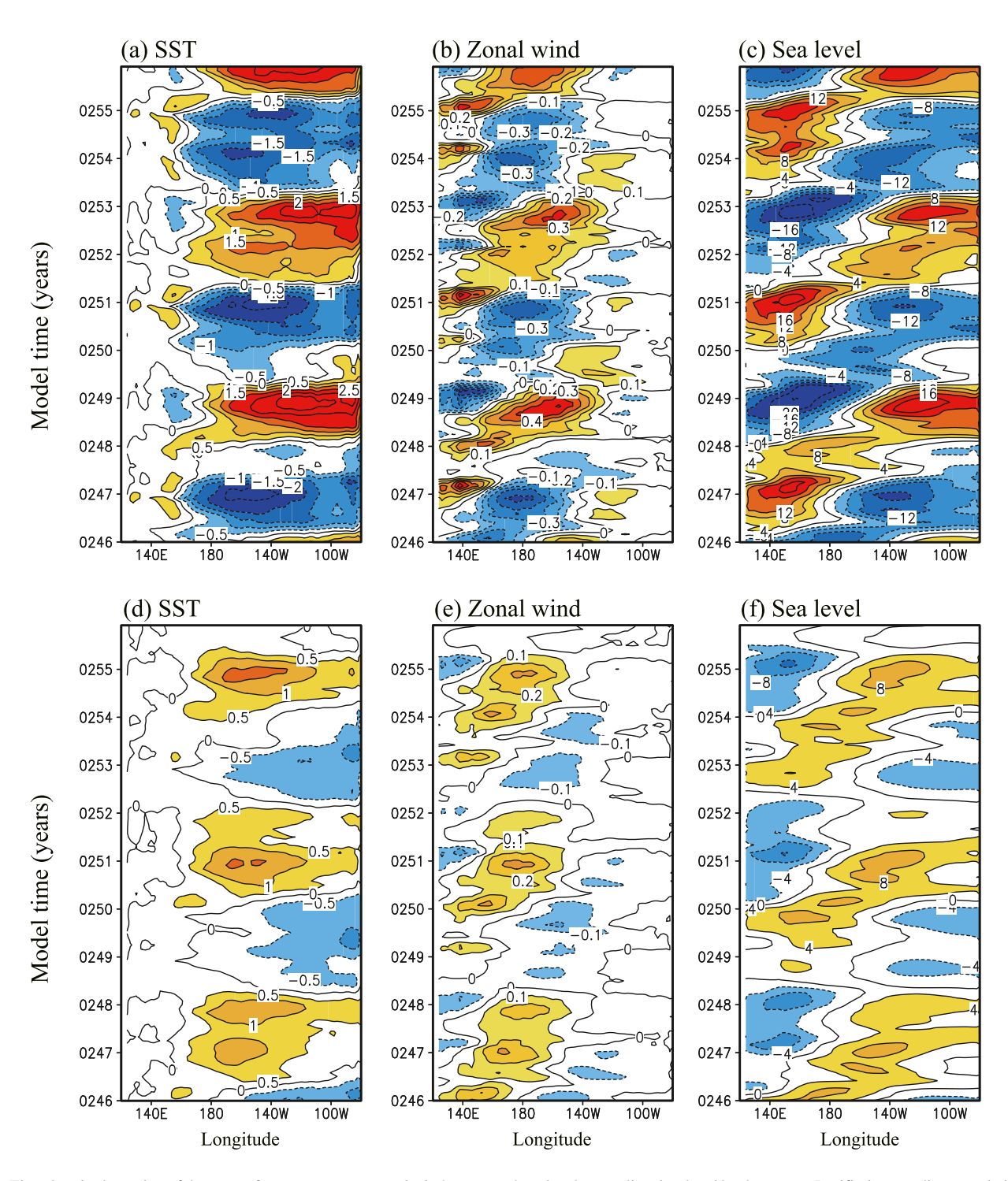


**Figure 2.** Time-longitude section of the sea surface temperature, zonal wind stress, and sea level anomalies simulated by the eastern Pacific-intermediate coupled climate model (EP-ICM) (upper panels) and central Pacific-ICM (lower panels). The contour intervals are 0.5°C in (a) and (d), 0.1 dyn/cm² in (b) and (e), and 4 cm in (c) and (f).

with the EP-OFV. Similarly, when the CP-OFV is applied, a CP El Niño-related model (hereafter termed CP-ICM) can be built.

To illustrate the performance of the reconstructed models in simulating different types of El Niño events, the simulations of the two models for key air-sea variables are presented in Figure 2 and Figures S1–S3 in Supporting Information S1. It can be seen that the SST evolutions simulated by the EP- and CP-ICMs are completely different

TAO AND DUAN 6 of 20

and have distinct dynamic characteristics as observed. For example, consistent with observations (Figure S1 in Supporting Information S1), the simulated EP El Niño is relatively intense with a warming center located further east of the tropical Pacific (Figure 2a). For the CP-ICM, the simulated SST of CP El Niño is relatively weaker and further west than that of EP El Niño simulated by the EP-ICM (Figure 2d). Besides the disparities in spatial structure, the simulated SST anomalies by the EP- and CP-ICMs also diverge in the temporal dimension. On the one hand, one strong CP El Niño event in the CP-ICM usually originates from cooling events in the EP and evolves into weaker warming events in the CP in the following year, whereas the strong EP El Niño event in the EP-ICM typically transitions into two consecutive years of cooling events in the CP. These results are all consistent with the observations and previous studies (Ashok et al., 2007; Z. Z. Hu et al., 2014; Kao & Yu, 2009; Tao & Duan, 2022), fully demonstrating the ability of the EP- and CP-ICMs to characterize the two types of El Niño events. Recently, Tao and Duan (2022) have observed that the EP cooling phenomenon is a precursor of CP El Niño events. However, they did not fully explore the reliability of this precursor and the underlying dynamic mechanisms. The CP-ICM developed in this study will provide an effective model platform for further verifying that EP-cooling is the optimal precursor for the onset of CP El Niño events.

Besides SST anomaly, the models are also capable of effectively characterizing the wind fields, ocean currents, and thermocline processes associated with different types of El Niño events (Figure 2 and Figures S2–S5 in Supporting Information S1). For instance, the EP-ICM well describes the eastward equatorial waves as indicated by the simulated SL anomaly. Compared to the air-sea state simulated by the EP-ICM, the westerly anomalies associated with the CP El Niño are confined to the western Pacific in the CP-ICM as well as the thermocline perturbations. As for the ocean current, although there are certain deviations between the model simulation and the observations, the overall characteristics are consistent with the observations. For example, consistent with the observation, the variability of zonal current anomalies during the CP El Niño event is mainly confined in the central tropical Pacific (Figures S2c and S2d in Supporting Information S1). In contrast, whatever in the observation or the EP-ICM simulation, the variability of zonal current anomalies during the EP El Niño event has a basin-scale pattern and is mainly located in the eastern tropical Pacific (Figures S2a and S2b in Supporting Information S1). Overall, the EP-ICM describes the EP El Niño events dominated by the basin-scale air-sea coupling processes, whereas the CP-ICM describes the CP El Niño events under the influence of local air-sea coupling processes.

Given the fact that the ICM itself has a relatively strong ability to characterize EP El Niño events, the optimized EP-ICM is expected to naturally simulate EP El Niño events that are closer to the observation. However, whether the CP-ICM can reasonably represent the air-sea coupling processes remains to be further verified, especially whether the dynamic mechanism of the transformation from EP-cooling to CP El Niño mentioned above is real and reasonable. To this end, we implement a composite analysis of 15 CP El Niño events simulated by the CP-ICM and explore the dynamic processes.

Figures 3 and 4 depict the spatiotemporal evolution of ocean-atmosphere variables during the transition from the EP-cooling phase to the CP El Niño with the CP-ICM. For comparison, results from observation are presented in Figures S4 and S5 in Supporting Information S1. Initially, the eastern tropical Pacific experiences a cooling phase that gradually weakens both in observation and model simulation. Concurrently, the warm SST in the boreal subtropical Pacific is progressively transferred to the central equator, eventually leading to the development of a CP El Niño event, of which processes have been revealed in previous studies (Ding et al., 2017; Kim et al., 2012; Tao & Duan, 2022). Specifically, in February the year before CP El Niño (i.e., February (-1) in Figure 3a), the EP-cooling phase is governed by basin-scale easterly anomalies near the equatorial Pacific, triggering anticyclonic wind anomalies in the central subtropical Pacific. In turn, these anticyclonic wind anomalies lead to an increase in SL anomaly and the accumulation of warm water near the dateline (Figure 4a). Subsequently, the ocean surface layer is warmed up. The boreal subtropical Pacific is thus characterized by the positive SST anomaly in December (-1) (Figure 3c). In observation, we can also observe the anticyclonic wind anomalies induced-SL anomalies near the dateline (Figures S5a-S5c in Supporting Information S1) and subsurface warming before the onset of CP El Niño. As the model simulates, a relatively weak warming phenomenon has been persisting in the boreal subtropical Pacific, although the SST anomaly in the region in the model simulation is stronger. Driven by the north equatorial counter current, the warm water propagates and diffuses eastward, counteracting the cold ocean (cold Rossby waves) transmitted from the EP. Meanwhile, the anticyclonic wind anomalies-induced SL anomalies propagate westward as warm Rossby waves. Blocked by the eastern Asian coast, the warm Rossby waves are reflected to deepen the thermocline in the western equatorial Pacific and trigger

TAO AND DUAN 7 of 20

21699291, 2025, 10, Downloaded from https://agupubs.onlinelibrary.wiley.com/doi/10.1029/2025JC022777 by Wansuo Duan-

Institution Of Atmospheric Physics, Wiley Online Library on [21/10/2025]. See the

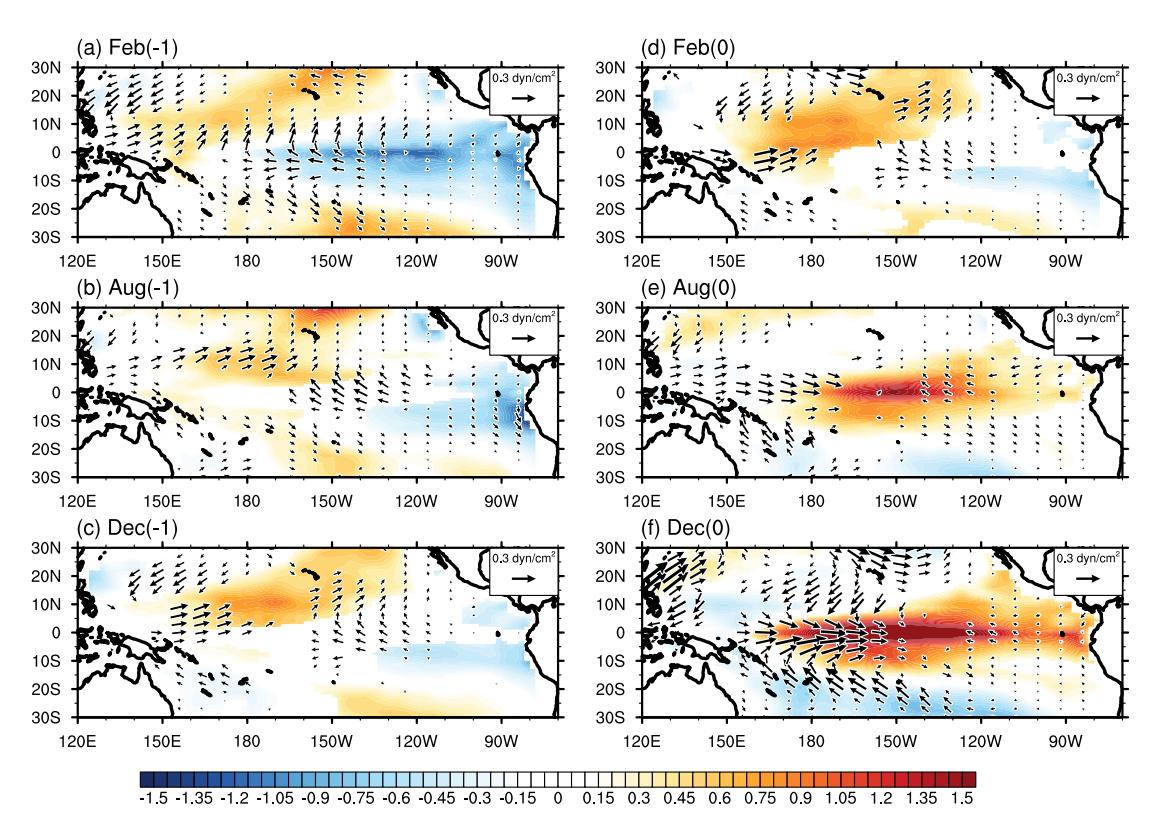


**Figure 3.** Evolutions of the central Pacific (CP) El Niño-related wind (vector) and sea surface temperature anomalies (shaded) simulated by the CP-intermediate coupled climate model. Only results that pass the 99% significance test are shown. The year of CP El Niño and the year before it are denoted as 0 and -1, respectively.

downwelling-Kelvin waves (Figure 4d), which is also reflected in observation (Figure S5d in Supporting Information S1). The EP-cooling phase gradually subsides under the influence of these two warming processes. At this moment, the eastern tropical Pacific exhibits a dipole SST pattern that couples with the wind anomaly to generate a Pattern of Pacific Meridional Mode -like structure (Figure 3d and Figure S4d in Supporting Information S1). Despite the relatively weak positive SST anomaly in the western Pacific, due to the instability of the air-sea coupling in spring, strong surface westerly anomalies are excited. In August (0), a significant warming in the central equatorial Pacific occurs (the SL anomaly is greater than 8 cm in Figure 4e and Figure S5e in Supporting Information S1). At this point, the difference in the SST anomaly between the central and western Pacific leads to an abnormal east-west gradient of the SL pressure and facilitates the maintenance of weak easterlies in the EP. Together with the westerly anomalies in the western Pacific, the wind field converges anomalously in the equatorial CP. As can be seen in Figures 4e and 4f of the model simulation and Figures S5e and S5f in Supporting Information S1 of the observation, a large amount of warm water converges and accumulates in the CP, leading to the development of a CP El Niño event.

Based on the above analysis, it is fully confirmed that the CP-ICM has the capability for CP El Niño evolution. Moreover, the dynamic mechanisms involved in the development of CP El Niño depicted by the model are consistent with previous studies (Ding et al., 2015; Stuecker, 2018; Tao & Duan, 2022; Vimont et al., 2014). For example, the surface air-sea coupling in the subtropical Pacific before the CP El Niño peaks, which is an important process for the onset of CP El Niño documented by Ding et al. (2015, 2017), can be well reproduced using the CP-ICM. Therefore, the CP-ICM can provide a brand-new model platform for the study of CP El Niño. Next, based on the CP-ICM, we will further explore the different roles of wind forcing and thermocline effects during the development of CP-El Niño.

TAO AND DUAN 8 of 20

21699291, 2025, 10, Downloaded from https://agupubs.onlinelibrary.wiley.com/doi/10.1029/2025JC022777 by Wansuo Duan-

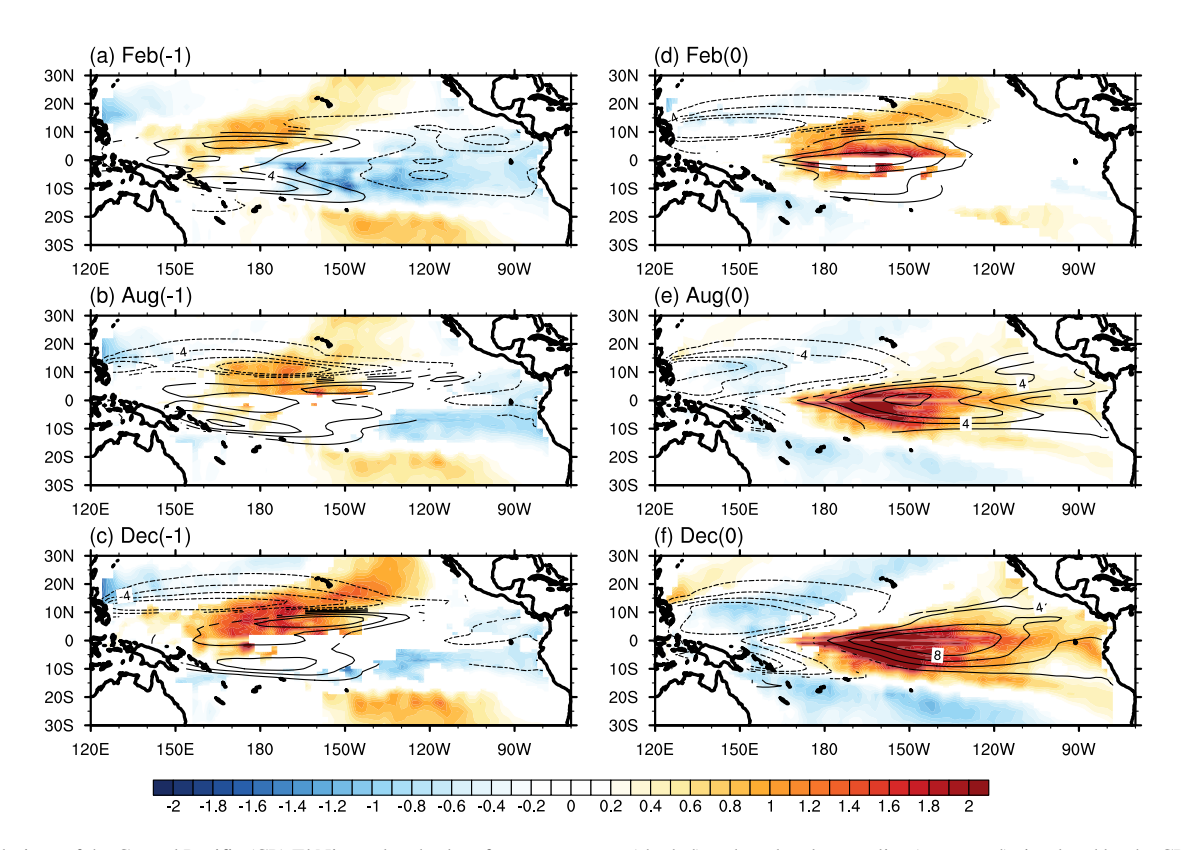


Figure 4. Evolutions of the Central Pacific (CP) El Niño-related subsurface temperature (shaded) and sea level anomalies (contoured) simulated by the CP-intermediate coupled climate model. Only results that pass the 99% significance test are shown. The contour interval is 2 cm.

#### 4. The Impact of Wind Forcing and Thermocline Effects on CP El Niño Simulation

#### 4.1. Experiment Design

As important sources of momentum and heat adjustment in the ocean, wind forcing, and thermocline perturbations play a crucial role in the traditional ENSO cycle. Previous studies have indicated that wind forcing and thermocline effects also play significant roles in the development of CP El Niño. However, controversies still persist in research on the individual contributions of wind forcing and the thermocline effect along with their relative roles in the development of CP El Niño events (Chung & Li, 2013; Fang & Mu, 2018; Fedorov et al., 2015; S. N. Hu et al., 2014; Lai et al., 2015; Zhi et al., 2019). Here, we will attempt to use the constructed CP-ICM to explore the impact on the simulation of the SST anomaly related to CP El Niño by altering the strengths of the wind forcing and thermocline effects.

The experiments are designed as follows. First, select a reference CP El Niño event. As the development of simulated CP El Niño is relatively similar, we select the model year 250 CP El Niño as the reference state and simulate the CP El Niño for 12 months starting from January of year 250 as the control experiment. Then, under the premise of ensuring that other structures of the model remain constant, the parameter related to the wind forcing effect in the model is adjusted. Note that the wind stress is a statistical function of SST in the ICM (Equation 1). The parameter  $\alpha_{\tau}$  represents the relative intensity of wind stress forcing on the ocean and the feedback intensity on SST. Therefore, we change the intensity of the wind forcing effect only by directly adjusting the parameter  $\alpha_{\tau}$  from 80% to 120% (in intervals of 5%) of its reference value. Besides, as revealed in Equation 2, we also change the parameter  $\alpha_{Te}$  (from 80% to 120% of the original value) to evaluate the impact of the thermocline effect on the CP El Niño simulation. Finally, by adjusting the relative magnitudes of  $\alpha_{\tau}$  and  $\alpha_{Te}$ , a set of 12-month simulations starting from January of the 250th year is carried out with the same initial condition. Including the control experiment, a total of  $9 \times 9 = 81$  groups of simulation experiments are conducted. By comparing the results of these experiments, the sensitivity of the model to these two parameters during the development of CP El Niño can be investigated.

TAO AND DUAN 9 of 20

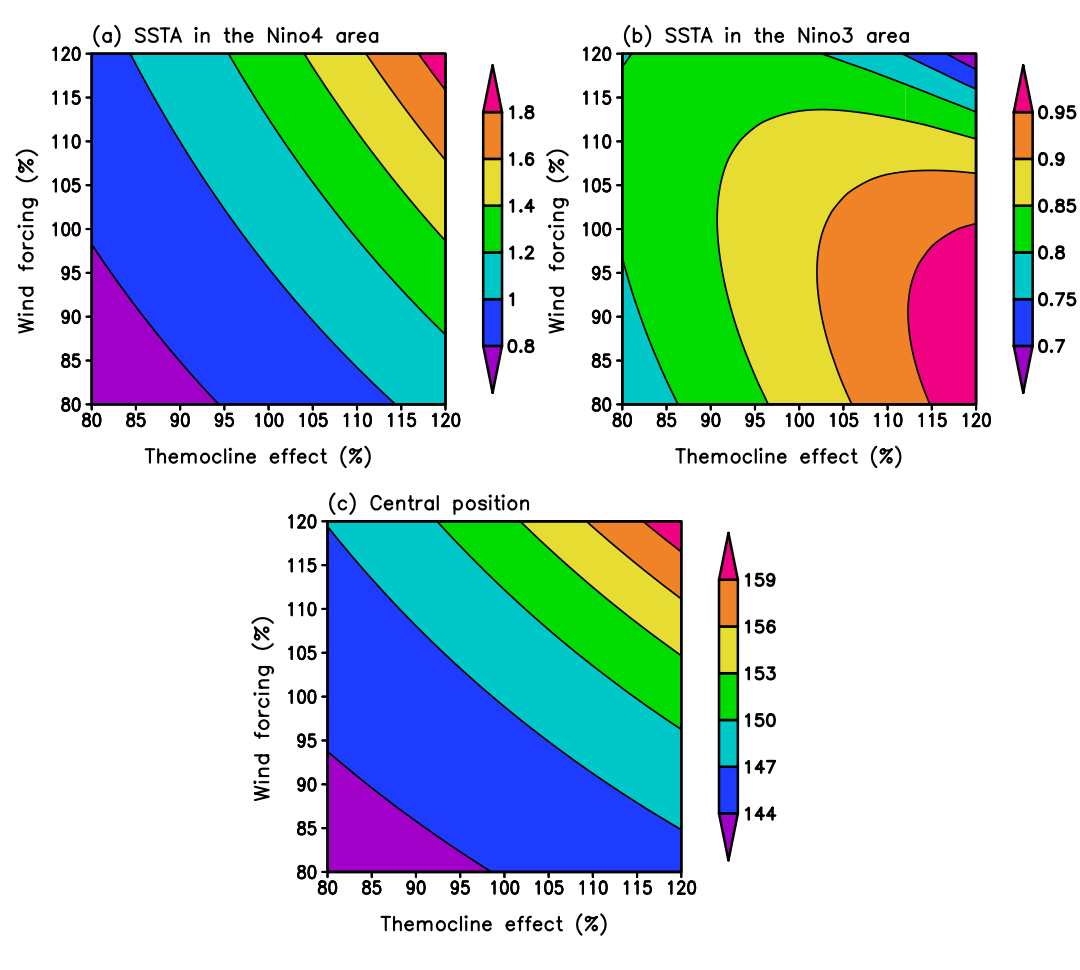


Figure 5. (a) Niño4 indices, (b) Niño3 indices, and (c) HCIs during the mature phase of the simulated Central Pacific El Niño as a function of the strength of the wind and thermocline effect. The contour intervals are 0.2°C in (a), 0.05°C in (b), and 3°W in (c).

#### 4.2. Nonlinearity of Wind Forcing and Thermocline Effects

To quantify the role of the wind forcing and thermocline effects in the horizontal distribution of the SST anomaly, a Heat Centre Index (HCI) is usually adopted to define the position of the warm center (Fedorov et al., 2015). The HCI is defined as  $HCI = \frac{\int_{xSSTA(x)} dx}{\int_{SSTA(x)} dx}$ , where the negative SST anomaly is set to zero during the calculation. Figure 5c shows the HCI of El Niño simulated under different intensities of wind forcing and thermocline effects. Note that the larger the HCI, further westward the warm center is located. It is clearly seen that enhancing the wind forcing and thermocline effects both cause the warm center of the simulated CP El Niño to shift westward. It seems to indicate that their effects on the SST anomaly simulation are equivalent. However, the actual situation is not that simple.

Figures 5a and 5b show the winter Niño4 and Niño3 indices in the CP El Niño simulation under the different strengths of the thermocline and wind forcing effects, respectively. It can be found that the Niño4 index exhibits a near-linear increase as the intensities of wind forcing and thermocline effects increase. However, the Niño3 index representing the SST anomaly in the EP exhibits a nonlinear response characteristic to the wind forcing and thermocline effects. Particularly, the increased thermocline effect promotes warming in the EP when the wind forcing effect is weak. But when the wind forcing effect is strong, an increase in the intensity of the thermocline effect actually has a cooling effect on the EP. Regarding the intensity of the wind forcing effect, whether in a system with a strong or weak thermocline effect, its effect on the SST anomaly in the EP is the same. As the wind forcing effect increases, it first warms the EP Ocean and then turns into a cooling effect.

TAO AND DUAN 10 of 20

Cases	Parameters	Meaning
0	$\alpha_{Te}:80\%, \alpha_{\tau}:80\%$	Mixed like-El Niño event
W	$\alpha_{Te}$ : 80%, $\alpha_{\tau}$ : 120%	Wind forcing-dominant CP El Niño
T	$\alpha_{Te}:120\%, \alpha_{\tau}:80\%$	Thermocline-dominant CP El Niño
С	$\alpha_{Te}$ : 120%, $\alpha_{\tau}$ : 120%	CP El Niño jointly dominated by both strong wind forcing and thermocline effects

Given the differences in the roles of wind forcing and thermocline effects in the simulation of the SST anomaly in the tropical Pacific, the scientific issues that urgently need to be addressed are: What specific impacts do the two have on CP El Niño respectively? Why is the response of Niño3 nonlinear? And through what specific processes do they cause the increase of the SST anomaly in the CP?

#### 4.3. Mechanisms of Central Pacific Warming Dominated by Wind Forcing and Thermocline Effects

To address the previous issues, we defined CP El Niño events under different forcing controlled-cases according to the intensities of thermocline effect and wind forcing effect (Table 1). In Figure 5c, when both the intensity of the wind forcing effect and that of the thermocline effect reach 80%, the warm center is located more to the east, resulting in the simulation being closer to Mixed-El Niño rather than CP El Niño (Strictly, it is neither CP nor EP El Niño). We define this case as the O event. When the intensity of the wind forcing effect is 80% and that of the thermocline effect is 120%, the position of the warm center is similar to that in the control experiment. In this case, the simulated CP El Niño event is dominated by the thermocline effect defined as a T (Thermocline-dominant CP El Niño) event. Conversely, when the intensity of wind forcing effect is 120% and that of the thermocline effect intensity is 80%, the simulated CP El Niño event is primarily controlled by the strong wind effect, which thus is defined as a W (Wind-dominant CP El Niño) event. When both the intensity of the wind forcing and thermocline effect reach 120%, the strongest CP El Niño event is simulated. This event is jointly influenced by both feedbacks and is defined as a C (Combined CP El Niño) event.

By comparing the air-sea evolutions of El Niño in W and O cases with the CP-ICM, we can analyze the impact of enhanced wind forcing on the simulation of CP El Niño. Comparing T and O cases allows us to analyze the impact of the enhanced thermocline effect. Therefore, to intuitively compare the impacts brought about by the changes in the two types of feedback, we calculated the differences between the simulation in W, T, and C cases and those of the O case. Regardless of whether it is the enhancement of wind forcing or thermocline effect, we find that the variation patterns of SST and wind anomaly are remarkably similar in the central tropical Pacific (Figure 6 and Figures S6 and S7 in Supporting Information S1). Both can lead to an elevation in the SST anomaly near the dateline, thereby simulating a strong CP El Niño event with the warming center located further west. In contrast, the effects of the strengthened wind forcing and thermocline effect on the eastern tropic vary among the three cases: compared with the O case, the EP experiences significant cooling in the W and C cases, but it undergoes slight warming in the T case.

To quantitatively analyze the differences in ocean process adjustments under these cases, we calculated the changes in ocean heat budget terms over 12-month simulations from the O case to the W/T/C case, as shown in Figure 7. It can be found that, regardless of whether the warming in the CP is caused by the enhancement of wind forcing or thermocline effect, there exists a significant enhancement of the vertical convection term in the CP leading to an increase in the Niño4 index. Specifically, the intensification of the vertical convection process is the primary oceanic heat transport process contributing to the warming in the CP. In contrast, the adjustment of the horizontal advection process exhibits a cooling effect in the EP. The warming effect in the central tropical Pacific and the cooling effect in the eastern tropical Pacific together cause the warm center of the simulated CP El Niño to shift westward.

It should be noted that, according to previous studies, the zonal advection feedback  $(-u'\frac{\partial \overline{I}}{\partial x})$  plays an important role in the development of CP El Niño. However, the present study shows that the horizontal advection process hardly plays a role in the growth of the SST anomaly in the central tropical Pacific during the development of CP

TAO AND DUAN 11 of 20

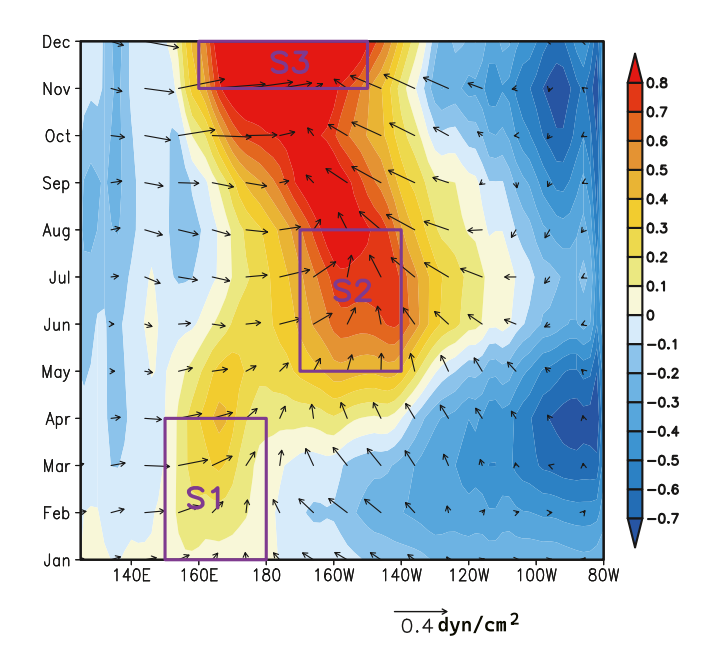


**Figure 6.** Differences in the sea surface temperature and wind stress anomalies between C and O cases. The box denotes three stages of the significant warming evolution, which is used to calculate the changes in the heat budget terms during different stages shown in Figures 10–12.

El Niño but shows a strong cooling effect in the EP (red bars in Figure 7). It seems to indicate that the zonal advection feedback is not a key mechanism for the CP El Niño in the model. In fact, it is not the case. Temporally, the zonal advection contributes to the change in the SST tendency in the CP from January to April and from August to December, whereas its contribution to the change in the EP occurs from April to July (Figure S8 in Supporting Information S1).

Hence, when attention is paid to the temporal evolution of the heat budget terms, it is found that the oceanic dynamic processes are different between the wind-dominant W case and the thermocline-dominant T case (e.g., Figure 8). The correlation between the changes in the tendency of SST anomaly and those in the zonal advection indicates that the enhanced CP El Niño in W and C cases is significantly related to the zonal advection (Figure S9a in Supporting Information S1). In contrast, the enhanced CP El Niño in the T case is related to the vertical convection (Figure S9b in Supporting Information S1). Figure 8 further shows the correlations to linear terms of the zonal advection and vertical convection terms (i.e.,  $-u' \cdot \frac{\partial \overline{T}}{\partial x}$ ,  $-\overline{u} \cdot \frac{\partial T'}{\partial x}$ ,  $-w' \cdot \frac{\partial \overline{T}}{\partial z}$ ,  $-\overline{w} \cdot \frac{\partial T'}{\partial z}$ ). It is demonstrated that the roles of terms of  $-\overline{u} \cdot \frac{\partial T'}{\partial x}$  and  $-w' \cdot \frac{\partial \overline{T}}{\partial z}$  on the SST evolution are identical among different cases, but roles of the zonal advection feedback  $(-u' \cdot \frac{\partial \overline{T}}{\partial x})$  and thermocline feedback  $(-\overline{w} \cdot \frac{\partial T'}{\partial z})$  are distinct. Specifically, the change in the zonal advection feedback primarily governs the CP warming in the W case, whereas the thermocline feedback plays the role in the T case.

When attention is paid to the EP, it appears that the correlations between the vertical convection or horizontal advection processes and the evolution of SST tendency in the EP do not differ significantly under different cases (Figure 8). It is indicated that the nonlinear response of the SST anomaly in the eastern tropical Pacific is irrelevant to these two oceanic processes. By analyzing the changes in the oceanic advection processes (Figure 9 and Figure S8 in Supporting Information S1), we find that it is the meridional advection that causes the trajectories of the SST anomaly in the eastern tropical Pacific to vary between the T and W cases. Specifically, the anomalous meridional advection by the climatological current  $(-\bar{\nu}\frac{\partial T'}{\partial y})$  acts as the main mechanism for sustaining the warming in the eastern tropical Pacific in the W case whereas the anomalous meridional advection by the

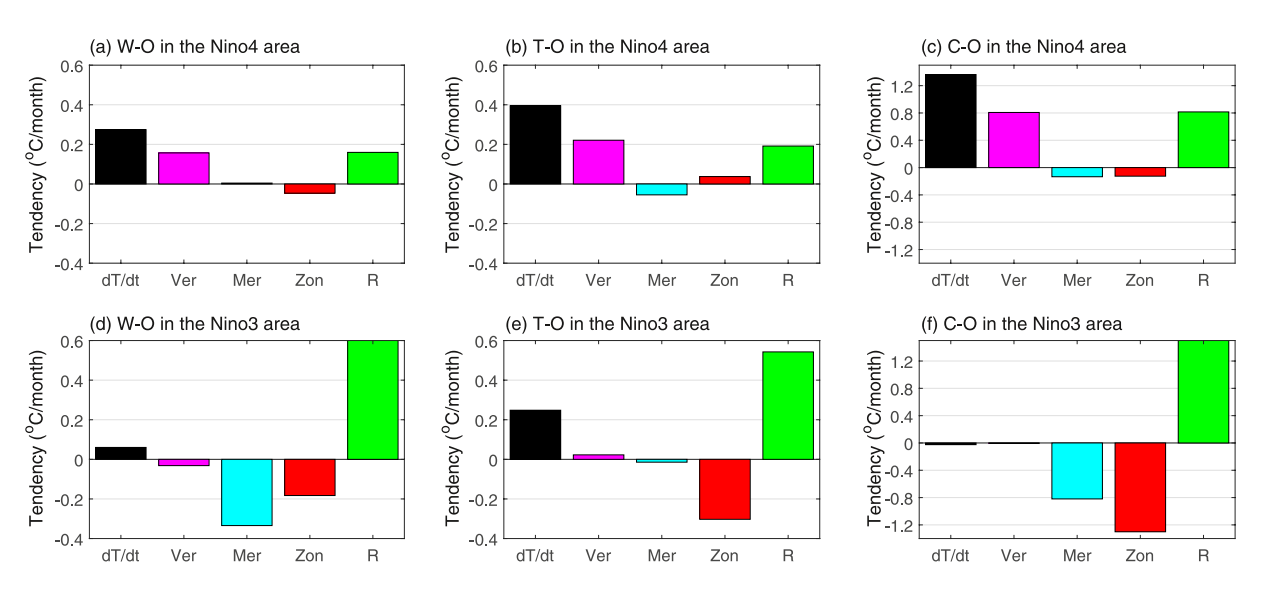


**Figure 7.** Changes in heat budget terms over 12-month simulations from case O to cases W, T, and O. The upper panels are calculated in the Niño4 region, and the lower panels are calculated in the Niño3 region. The ticks of the *x*-coordinate are the terms of the tendency of the sea surface temperature anomaly, vertical convection, meridional advection, zonal advection, and residual term.

TAO AND DUAN 12 of 20

21699291, 2025, 10, Downloaded from https://agupubs.onlinelibrary.wiley.com/doi/10.1029/2025IC022777 by Wansuo Duan -

Institution Of Atmospheric Physics, Wiley Online Library on [21/10/2025]. See the Term

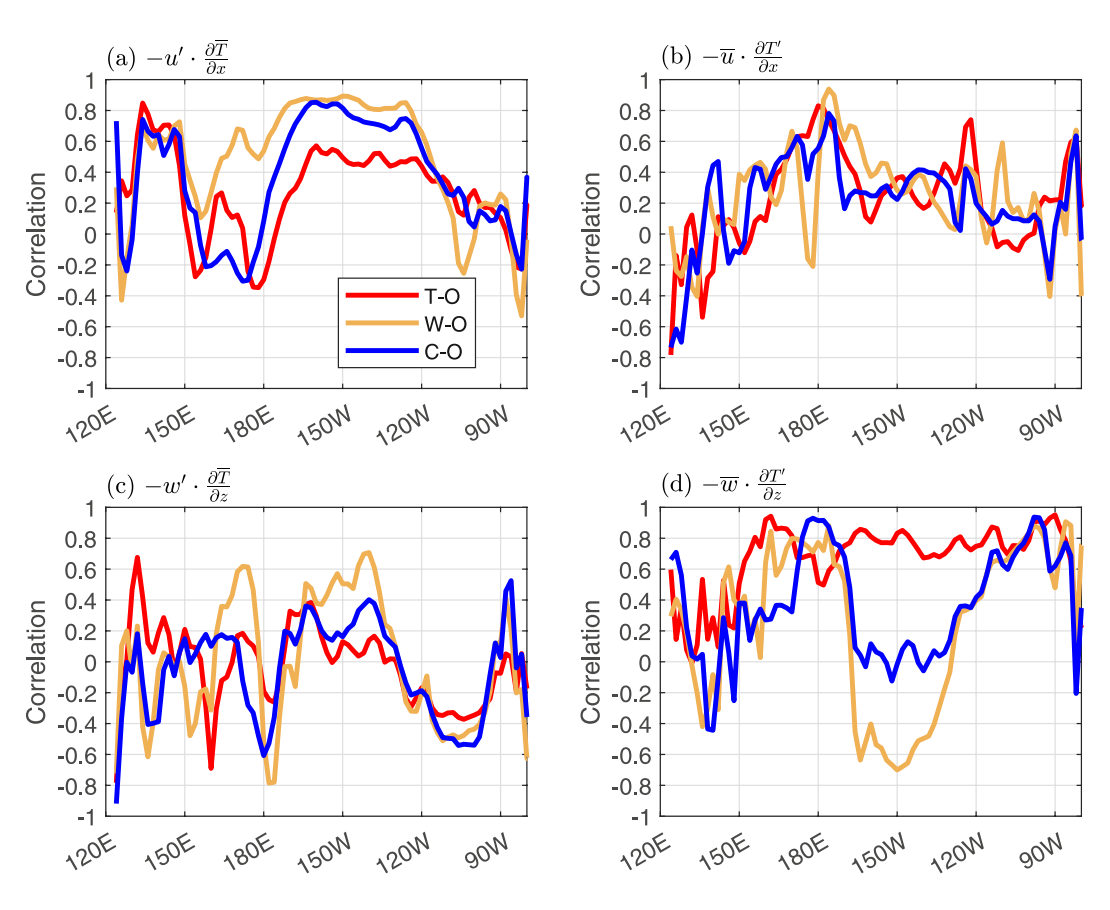


**Figure 8.** Correlations of the changes in the tendency of sea surface temperature anomaly to the changes in the linear zonal advection and vertical convection terms along the equator.

anomalous current  $(-v' \cdot \frac{\partial \overline{I}}{\partial y})$  controls the cooling effect in the eastern tropical Pacific in the T case. That is, the nonlinear response of the SST anomaly in the eastern tropical Pacific to the changes in the strengths of the wind forcing and thermocline effects is dynamically due to the distinct role played by the meridional convection.

Another phenomenon worthy of attention in Figure 6 is that the impacts of wind forcing and thermocline effects on the warming in the CP go through three stages, namely the initial warming stage (S1), the rapid warming stage (S2), and the warming maintenance stage (S3). Moreover, whether the wind forcing or the thermocline effect is enhanced in the CP-ICM, the CP experiences these three stages. Hence, we further analyze the similarities and differences in the adjustments of ocean processes by wind forcing and thermocline effect in different stages (Figures 9–11).

Figure 10 clearly shows that the ocean processes leading to the initial warming in stage S1 vary under different cases. In the W case, the intensification of the zonal advection process stands as the most crucial oceanic heat-transport mechanism contributing to the rapid initial warming in the CP (Figure 10a, red bar). Although in the T case, besides the zonal advection process, the intensification of the vertical convection process also serves as a significant factor driving the rapid warming in Stage S1 (Figure 10b, pink bar). During the onset of CP El Niño i.e. dominated by the wind forcing (i.e., W case), the westerly anomalies in the western equatorial Pacific are more likely to drive the ocean to generate an eastward anomalous current, which transports the warm water from the warm pool to the CP. As a result, the zonal advection plays a key role in stage S1. As to the CP El Niño event dominated by the thermocline, the effect of the thermocline is amplified and affects the surface layer through the vertical convection process, leading to intensified surface warming. One can also find that although the vertical convection process can promote ocean warming in the W case, its intensity is much lower than that in the T case. In the T case, the enhancement of the thermocline effect directly strengthens the vertical convection process. Meanwhile, the surface heated by the subsurface can couple with the atmosphere to generate a corresponding wind anomaly, which in turn acts on the zonal current. That is, the enhanced thermocline effect can project onto

TAO AND DUAN 13 of 20

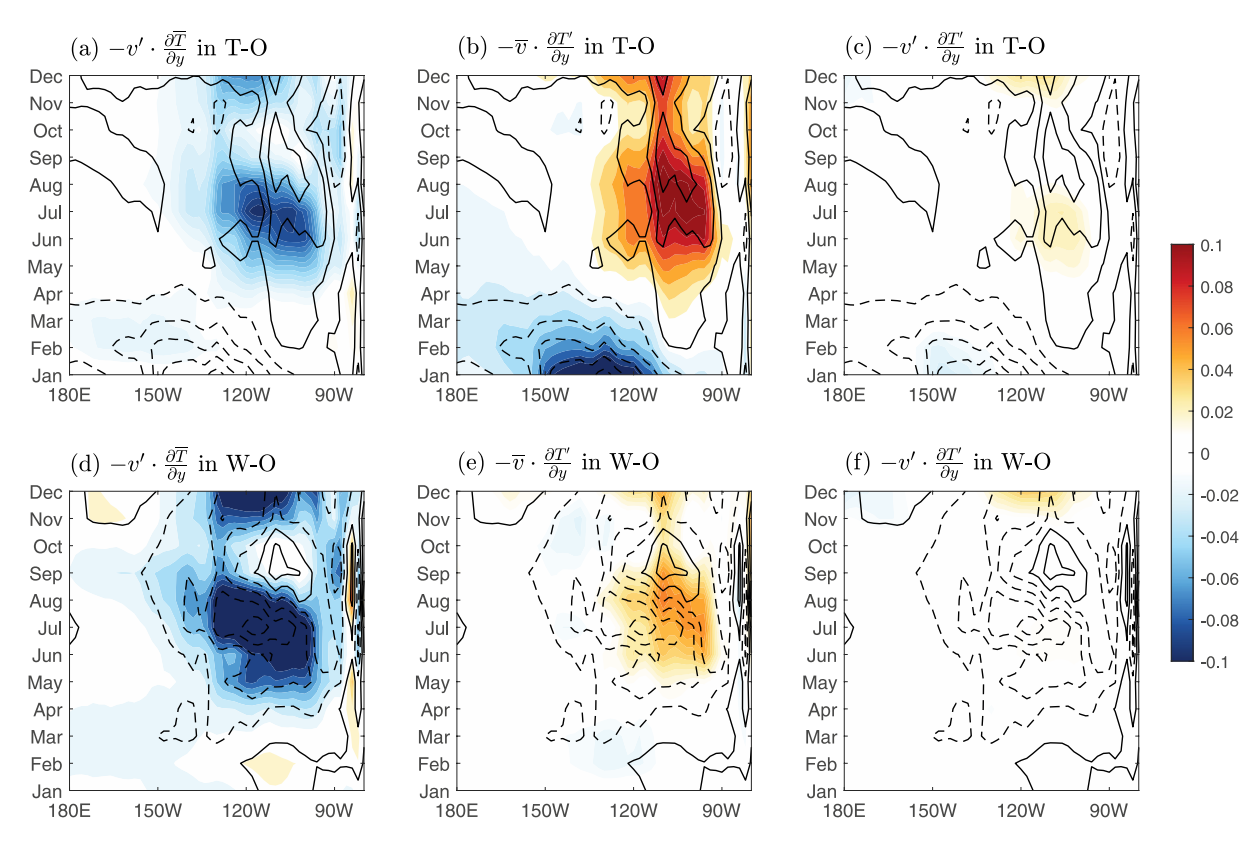
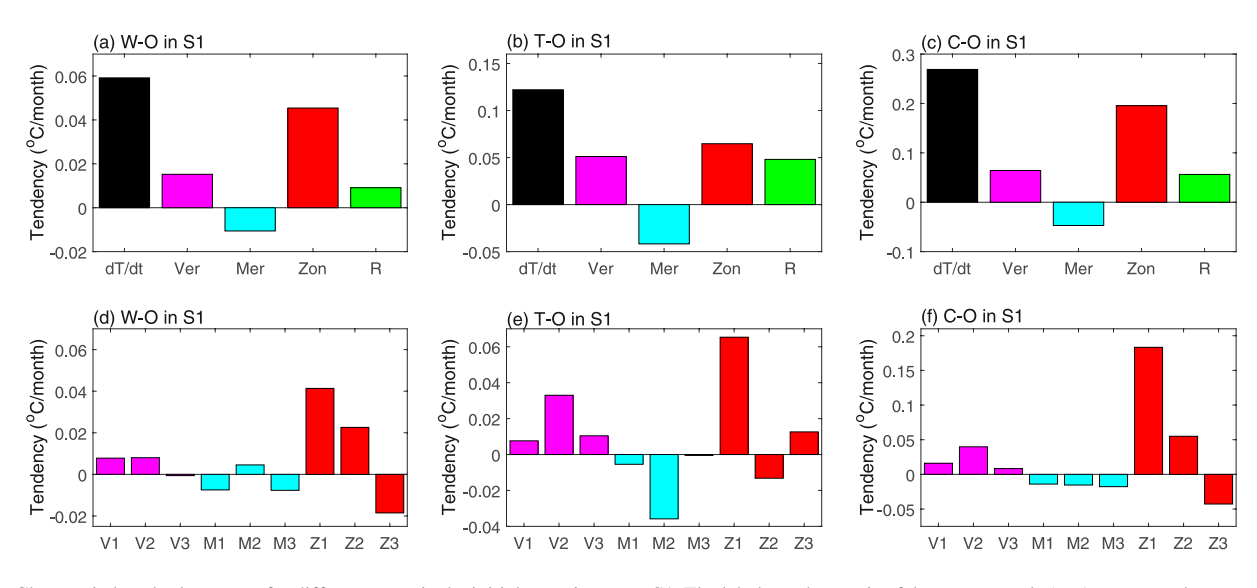


Figure 9. Changes in the meridional advection terms in the eastern equatorial Pacific for different cases. The component of the meridional advection is shaded. The total meridional advection is contoured, with a contour interval of 0.03°C/month.

the zonal current to change the zonal advection process. Therefore, whether it is the thermocline or the wind-dominated CP El Niño event, the zonal advection process plays a crucial role in the initial warming. Evidently, the zonal advection process is the most significant warming mechanism in the C case (Figure 10c).



**Figure 10.** Changes in heat budget terms for different cases in the initial warming stage S1. The labels on the *x*-axis of the upper panels (a–c) represent the terms related to the tendency of the sea surface temperature anomaly, vertical convection, meridional advection, zonal advection, and residual. The labels on the *x*-axis of the bottom panels (d–f) are the three sub-terms of the vertical convection  $(-w' \cdot \frac{\partial \overline{T}}{\partial z}, -\overline{w} \cdot \frac{\partial T'}{\partial z})$ , meridional advection  $(-v' \cdot \frac{\partial \overline{T}}{\partial y}, -\overline{v} \cdot \frac{\partial T'}{\partial y})$ , and  $-v' \cdot \frac{\partial T'}{\partial y}$  and zonal advection  $(-u' \cdot \frac{\partial \overline{T}}{\partial x}, -\overline{u} \cdot \frac{\partial T'}{\partial x}, -\overline{u} \cdot \frac{\partial T'}{\partial x})$ , and  $-u' \cdot \frac{\partial T'}{\partial x}$ .

TAO AND DUAN 14 of 20

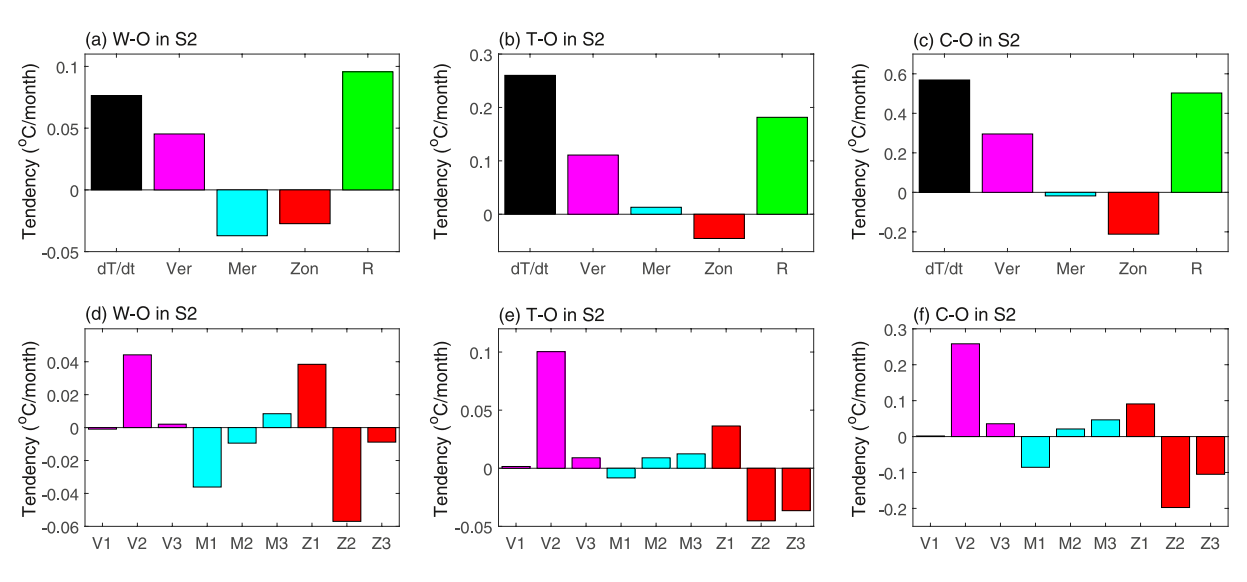


Figure 11. As in Figure 10, in the rapid warming stage S2.

When the horizontal advection and vertical convection processes are further decomposed, it can be found that the zonal advection feedback  $(-u' \cdot \frac{\partial \overline{T}}{\partial x})$  always plays the most crucial role in the initial warming stage (Figure 10d). In contrast, when the thermocline effect is enhanced, the thermocline feedback  $(-\overline{w} \cdot \frac{\partial T'}{\partial z})$  also strengthens accordingly, and its intensity is only second to that of the zonal advection feedback (Figure 10e).

Entering Stage S2, that is, spring and summer, the air-sea coupling is intense at this time. An anomalous convergent wind is excited in the central equatorial Pacific (Figure 6), which in turn triggers an anomalous downward current, leading to a rapid increase in SST in the CP. In the W case, with the enhancement of the wind forcing effect, it can be inferred that the resulting intensified downward current will cause further warming in the surface Pacific. Therefore, from the heat budget analysis, it can be observed that the enhancement of the vertical convection term dominates the rapid warming of the sea surface in S2 of the W case (Figure 11a). In the T case, with the enhancement of the thermocline effect, the anomalous warm subsurface water in spring and summer can more easily affect the surface layer, thereby accelerating the warming of the sea surface in S2 through the vertical convection process (Figure 11b). Thus, the vertical convection process is also the main oceanic heat-transport process that dominates the warming of the CP in the S2 of the T case. More precisely, the thermocline

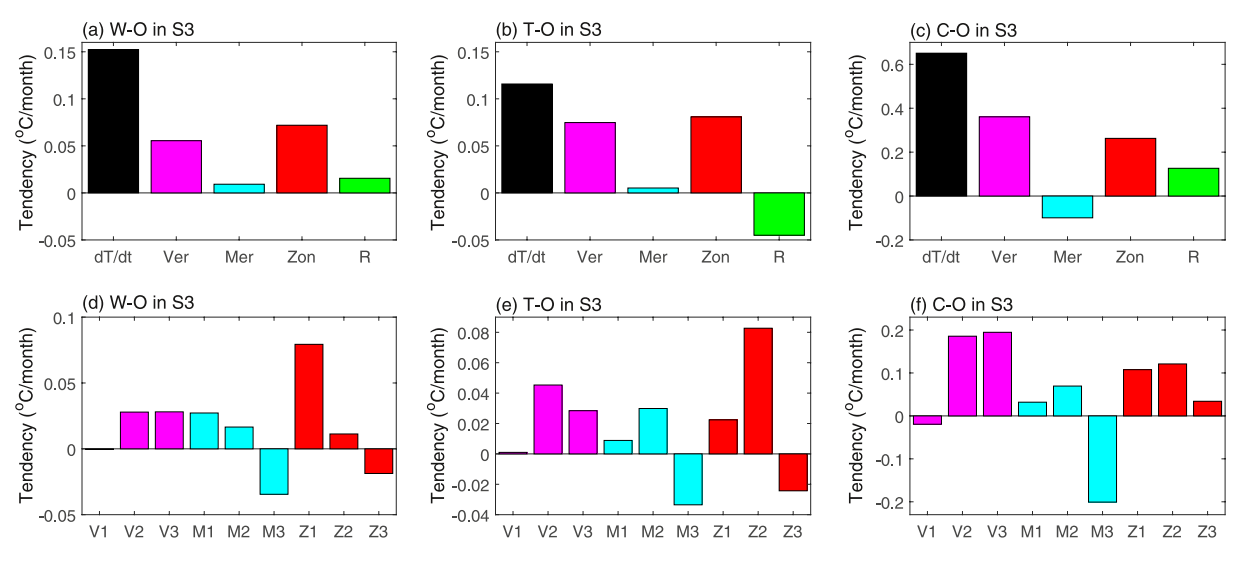


Figure 12. As in Figure 10, in the warming maintenance stage S3.

TAO AND DUAN 15 of 20

feedback  $(-\overline{w} \cdot \frac{\partial T'}{\partial z})$  in the vertical convection process dominates the rapid warming of the CP (Figures 11d and 11e). On the contrary, when the thermocline effect or the wind forcing effect is enhanced, the zonal advection process tends to inhibit the warming trend. However, when we decompose the horizontal advection process, we can find that the horizontal advection feedback  $(-u' \cdot \frac{\partial \overline{T}}{\partial x})$  term is still the warming mechanism second only to the thermocline feedback. In the C case, the warming effect of the thermocline feedback is more significant (Figure 11f).

In Stage S3, the CP El Niño undergoes a process of gradual maturation. Concurrently, the warming effects resulting from the intensification of wind forcing and thermocline effects start to wane. As depicted in Figure 12, it can be evident that in any case, the linear vertical convection process and the linear zonal advection process are the primary oceanic processes responsible for sustaining the warming. The distinction lies in the fact that in the W case, the zonal advection feedback emerges as the dominant term (Figure 12d). In contrast, in the T case, the anomalous zonal advection by the climatological current  $(-\overline{u} \frac{\partial T'}{\partial x})$  serves as the principal mechanism for sustaining the warming followed by the thermocline feedback (Figure 12e).

Overall, the wind forcing-dominated climate system mainly enhances the zonal advection feedback mechanism, making the simulated warm event located more westward to be a CP El Niño. The thermocline-dominated climate system not only enhances the zonal advection feedback but also strengthens the thermocline feedback, resulting in a rapid SST growth in the CP to be a CP El Niño.

#### 5. Summary and Discussion

As a crucial component of global climate variability, the evolution and variability of El Niño have always been a prominent topic in both the social and scientific communities. Since the beginning of this century, different from traditional EP El Niño events, CP El Niño events have occurred frequently, posing new challenges to understanding and predicting short-term climate change. Improving the climate model with the ability of simulating the El Niño diversity appears to be of particular importance. To overcome the effect of the model uncertainty, the present study employs the NFSV-assimilation approach to optimize an ENSO-related ICM. Based on the optimized model, we primarily investigate the dynamic mechanisms by which wind and the thermocline influence the development of CP El Niño.

The NFSV-assimilation method is a nontraditional approach that focuses on the model itself and attributes all model uncertainties to the SST model tendency equation of the ICM. By assimilating the observed SST anomaly from 1960 to 2020, a large number of monthly NOFVs are obtained. The NOFVs can force the ICM to reproduce the interannual variability of the SST in the tropical Pacific including the EP and CP El Niño. Therefore, in a sense, NOFVs can characterize physical processes that are absent or unsolved in the ICM. We then classify these NOFVs into two sets according to the El Niño type and obtain two types of NOFVs, namely CP-OFV and EP-OFV. In a sense, the CP- and EP-OFVs reflect the typical characteristics of missed dynamics in simulating CP and EP El Niño with the ICM, respectively.

Using the EP-OFV and CP-OFV in an annual-cycle form to drive the ICM respectively, two El Niño type-related models are successfully established: the EP-ICM and CP-ICM. The performances of both models are remarkable. They can accurately depict the spatial structure, amplitude, and zonal transitions of the EP and CP El Niño. In terms of the spatial structure, the EP-ICM simulates the EP El Niño with a warmer center located in the EP region, whereas the CP-ICM simulates a relatively weaker and more westward warm center for CP El Niño, which is consistent with observations (Ashok et al., 2007; Z. Z. Hu et al., 2014; Kao & Yu, 2009; Tao & Duan, 2022). In the temporal dimension, the models also capture the typical evolution patterns of different El Niño events. For instance, the strong CP El Niño event simulated by the CP-ICM originated from cooling events in the EP and evolved into weak warming events in the CP in the following year. In the EP-ICM, a strong El Niño event is usually followed by consecutive multiyear La Niña events.

Additionally, based on the CP-ICM, we examine the sensitivity of CP El Niño simulation to intensities of wind forcing and thermocline effects. A series of experiments is designed by adjusting the parameters related to wind forcing and thermocline effects in the CP-ICM. A total of 81 groups of sensitivity experiments are carried out. The SST anomaly in the EP exhibits a nonlinear response to the enhancement of wind forcing and thermocline effects. When the wind forcing effect increases, the simulated SST anomaly in the EP initially increases and then

TAO AND DUAN 16 of 20

meridional advection.

decreases. Recently, L. Geng and Jin (2023) also confirmed the nonlinearity of the SST anomaly in the eastern tropical Pacific. These results also imply the complexity of the oceanic processes in the EP. Further study reveals that the nonlinear response of the SST anomaly in the eastern tropical Pacific to the wind forcing is dynamically due to the meridional convection. As the wind forcing is enhanced, a stronger cross-equatorial current is generated to transport the cold water in the tropical southeastern Pacific to the equator, thereby cooling the EP through the

In contrast, the SST anomaly in the CP exhibits a near-linear increase as the intensities of wind forcing and thermocline effects increase. Hence, regardless of which forcing effect is enhanced, it will eventually result in a stronger CP El Niño. The evolutions of warming are similar, yet the underlying ocean processes vary. To quantify the warming mechanisms induced by the enhancements of wind forcing and thermocline effects, heat budget analyses are conducted among the developments of CP El Niño under different cases. In the wind-dominated climate system, the zonal advection feedback consistently assumes the most significant positive feedback process during different warming stages. The enhancement of the wind forcing effect makes the zonal current more easily driven by the wind, resulting in stronger eastward current anomalies and manifesting strong zonal advective feedback, thereby giving rise to rapid SST growth in the CP. In the thermocline-dominated climate system, both the zonal advection feedback and the thermocline feedback serve as crucial oceanic processes that accelerate the warming trend in the CP.

It should be emphasized that the findings of this study are mainly attributed to the extraction of the CP- and EP-OFV using the NFSV assimilation method. Although these NOFVs appear to be relatively straightforward, the physical processes they imply are extremely obscure due to the complexity and variability of model errors. That is to say, from a physical perspective, the exact nature of CP-OFV and EP-OFV remains unclear. They may be ascribed to the extratropical processes absent from the model along with the interactions among various spatiotemporal scales within the model. These unknown processes are very likely to be the crucial factors that change the patterns of El Niño. The wind forcing and thermocline effects involved in this study can only show that both of them can influence the strength of CP El Niño. What we are most concerned about is that the key factors for the transformation of CP and EP El Niño are hidden in these forcing vectors. It is particularly important to deeply explore the physical meaning behind NOFVs. Therefore, from the perspective of the dynamic framework, we will focus more on the physical processes represented by the NOFVs to achieve the goal of correcting the climate model by optimizing these physical process in the future.

Besides delving into the physical meanings of NOFVs, it is also worthy of attention to how to use NOFVs to improve predictions. Previous studies have documented that the model errors are flow-dependent. Therefore, based on the linear statistical relationship between SST and NOFVs, Tao and Duan (2019) first developed a new model that is to predict the model errors during the ENSO prediction. They then nested this model into the ICM to counteract the influence of model errors and thus improve the ENSO prediction skills. Differing from traditional post-correction schemes, the ocean-atmosphere processes in the ICM are adjusted simultaneously with the online correction process, thus achieving a better prediction within the air-sea coupling framework (Tao et al., 2020). In addition, by constructing statistical relationships between SST and NOFVs under different interdecadal backgrounds, the interdecadal predictability information can be captured, thereby further enhancing ENSO prediction skills (Zheng et al., 2023). From a mathematical perspective, the improvement in prediction is related to the established relationship between SST and NOFVs. Evidently, strengthening the relationship will further improve the prediction skill. Recently, the rise of deep learning technology has provided a highly reliable and effective method for constructing the nonlinear relationships between two physical variables. Take the convolutional neural network like U-NET as an example (Ronneberger et al., 2015). On the one hand, through convolution and pooling operations, the network can extract features at different scales from the input data. These features at different scales help the network understand information at different levels in the two spatial fields, thus more effectively establishing the relationship. On the other hand, through the combination of the contraction path and the expansion path, U-NET can learn representative features even with a small data set, which is very suitable for constructing relationships between climate variables with limited data. For instance, based on the U-NET framework, Du and Zhang (2024, 2025) successfully built the nonlinear relationship between wind and SST. They then replaced the original linear statistical model in the ICM with this new model, which effectively improved the ENSO simulation. It can be expected that, compared with traditional statistical methods, deep learning technology can more accurately capture the nonlinear relationship between NOFVs and oceanatmosphere variables. If one NOFVs-related error model constructed by deep learning is integrated into the

TAO AND DUAN 17 of 20 Acknowledgments

We extend our sincere gratitude to

anonymous reviewers for their invaluable

suggestions on this study. We would like to

Rong-Hua Zhang, Mu Mu, and Hai Zhi for

their guidance and support throughout this

convey our special thanks to Professors

study. This research was funded by the

National Natural Science Foundation of

Foundation for Introducing Talent of

China (42330111; 42405062), the Startup

NUIST, the Jiangsu Innovation Research

Group (JSSCTD 202346), and the Ministry

of Science and Technology of the People's

Republic of China (2020YFA0608802).

We thank for the technical support of the

National Large Scientific and

(https://cstr.cn/31134.02.EL).

Technological Infrastructure "Earth

System Numerical Simulation Facility"

dynamic model, it will effectively improve the model performance and further enhance ENSO prediction skills. Our research team is currently actively promoting this work and will announce the research results to readers as soon as possible. Besides, the derived CP-OFV and EP-OFV can also be used to improve the prediction of El Niño diversity (the discussion is given in Text S2 in Supporting Information S1).

Overall, the above results fully demonstrate that the NFSV-assimilation approach can improve the simulation and provide a critical foundation for enhancing the understanding and prediction of the El Niño diversity. Specifically, the ENSO model that we have developed for EP and CP El Niño events will offer a crucial modeling framework for the study of ENSO diversity.

#### **Conflict of Interest**

The authors declare no conflicts of interest relevant to this study.

#### **Data Availability Statement**

The monthly SST data during the period from 1960 to 2020 are obtained from the reconstructed SST data at NOAA (ERSSTv5; Huang et al., 2017; downloaded at https://doi.org/10.7289/V5T72FNM). The zonal and meridional currents during the period from 1980 to 2024 are obtained from the Global Ocean Data Assimilation System (GODAS) reanalysis (Behringer et al., 1998; downloaded at https://psl.noaa.gov/data/gridded/data.godas.html). All scripts used to analyze the data and generate the figures are written using the GrADS 2.2.1 (https://github.com/j-m-adams/GrADS) software and MATLAB 2018b (Morel, 2018).

#### References

- Ashok, K., Behera, S. K., Rao, S. A., Weng, H. Y., & Yamagata, T. (2007). El Niño Modoki and its possible teleconnection. *Journal of Geophysical Research*, 112(C11), C11007. https://doi.org/10.1029/2006jc003798
- Battisti, D. S. (1988). Dynamics and thermodynamics of a warming event in a coupled tropical atmosphere ocean model. *Journal of the Atmospheric Sciences*, 45(20), 2889–2919. https://doi.org/10.1175/1520-0469(1988)045<2889:Datoaw>2.0.Co;2
- Behringer, D. W., Ji, M., & Leetmaa, A. (1998). An improved coupled model for ENSO prediction and implications for ocean initialization. Part I: The ocean data assimilation system. *Monthly Weather Review*, 126, 1013–1021. https://doi.org/10.1109/ISEMC.2006.1706326
- Capotondi, A. (2013). ENSO diversity in the NCAR CCSM4 climate model. *Journal of Geophysical Research: Oceans*, 118(10), 4755–4770. https://doi.org/10.1002/jgrc.20335
- Chen, D. K., Lian, T., Fu, C. B., Cane, M. A., Tang, Y. M., Murtugudde, R., et al. (2015). Strong influence of westerly wind bursts on El Niño diversity. *Nature Geoscience*, 8(5), 339–345. https://doi.org/10.1038/Ngeo2399
- Chen, M. Y., Yu, J. Y., Wang, X., & Chen, S. (2021). Distinct onset mechanisms of two subtypes of CP El niño and their changes in future warming. Geophysical Research Letters, 48(14), e2021GL093707. https://doi.org/10.1029/2021GL093707
- Chen, N., & Fang, X. (2023). A simple multiscale intermediate coupled stochastic model for El Niño diversity and complexity. *Journal of Advances in Modeling Earth Systems*, 15(4), e2022MS003469. https://doi.org/10.1029/2022MS003469
- Chen, N., Fang, X., & Yu, J. Y. (2022). A multiscale model for El Niño complexity. npj Climate and Atmospheric Science, 5(1), 16. https://doi.org/
- 10.1038/s41612-022-00241-x
  Chen, N., & Majda, A. J. (2016). Simple dynamical models capturing the key features of the Central Pacific El Niño. *Proceedings of the National*
- Academy of Sciences, 113(42), 11732–11737. https://doi.org/10.1073/pnas.1614533113

  Choi, J., An, S. I., Kug, J. S., & Yeh, S. W. (2011). The role of mean state on changes in El Nio's flavor. Climate Dynamics, 37(5–6), 1205–1215. https://doi.org/10.1007/s00382-010-0912-1
- Chung, P. H., & Li, T. (2013). Interdecadal relationship between the mean state and El Niño types. *Journal of Climate*, 26(2), 361–379. https://doi.org/10.1175/Jcli-D-12-00106.1
- Ding, R. Q., Li, J. P., Tseng, Y. H., Sun, C., & Guo, Y. P. (2015). The Victoria mode in the North Pacific linking extratropical sea level pressure variations to ENSO. *Journal of Geophysical Research: Atmospheres*, 120(1), 27–45. https://doi.org/10.1002/2014jd022221
- Ding, R. Q., Li, J. P., Tseng, Y. H., Sun, C., & Zheng, F. (2017). Linking a sea level pressure anomaly dipole over North America to the central Pacific El Niño. Climate Dynamics, 49(4), 1321–1339. https://doi.org/10.1007/s00382-016-3389-8
- Du, S., & Zhang, R.-H. (2024). An RCUNet-based sea surface wind stress model with multi-day time sequence information incorporated and its applications to ENSO modeling. *Ocean Modelling*, 194, 102500. https://doi.org/10.1016/j.ocemod.2025.102500
- Du, S., & Zhang, R.-H. (2025). U-net models for representing wind stress anomalies over the tropical Pacific and their integrations with an intermediate coupled model for ENSO studies. Advances in Atmospheric Sciences, 41(7), 1403–1416. https://doi.org/10.1007/s00376-023-3179-2
- Duan, W. S., Tian, B., & Xu, H. (2014). Simulations of two types of El Niño events by an optimal forcing vector approach. *Climate Dynamics*, 43(5–6), 1677–1692. https://doi.org/10.1007/s00382-013-1993-4
- Fang, X. H., Dijkstra, H., Wieners, C., & Guardamagna, F. (2024a). A nonlinear full-field conceptual model for ENSO diversity. *Journal of Climate*, 37(14), 3759–3774. https://doi.org/10.1175/Jcli-D-23-0382.1
- Fang, X. H., Dijkstra, H., Wieners, C., & Guardamagna, F. (2024b). An overlooked aspect concerning the effect of the spatial pattern of zonal wind stress anomalies on El Niño evolution and diversity. Climate Dynamics, 62(8), 7037–7047. https://doi.org/10.1007/s00382-024-07264-5
- Fang, X. H., & Mu, M. (2018). Both air-sea components are crucial for El Niño forecast from boreal spring. Scientific Report UK, 8(1), 10501. https://doi.org/10.1038/s41598-018-28964-z
- Fedorov, A. V., Hu, S. N., Lengaigne, M., & Guilyardi, E. (2015). The impact of westerly wind bursts and ocean initial state on the development, and diversity of El Niño events. Climate Dynamics, 44(5–6), 1381–1401. https://doi.org/10.1007/s00382-014-2126-4

TAO AND DUAN 18 of 20

- Feng, J., Lian, T., Ying, J., Li, J. D., & Li, G. (2020). Do CMIP5 models show El Niño diversity? *Journal of Climate*, 33(5), 1619–1641. https://doi.org/10.1175/Jcli-D-18-0854.1
- Geng, L., & Jin, F. F. (2023). Insights into ENSO diversity from an intermediate coupled model. Part II: Role of nonlinear dynamics and stochastic forcing. *Journal of Climate*, 36(21), 7527–7547. https://doi.org/10.1175/JCLI-D-23-0044.1
- Geng, T., Cai, W., & Wu, L. (2020). Two types of ENSO varying in tandem facilitated by nonlinear atmospheric convection. *Geophysical Research Letters*, 47(15), e2020GL088784. https://doi.org/10.1029/2020GL088784
- Ham, Y. G., & Kug, J. S. (2012). How well do current climate models simulate two types of El Niño? Climate Dynamics, 39(1–2), 383–398. https://doi.org/10.1007/s00382-011-1157-3
- Hou, M. Y., & Tang, Y. M. (2022). Recent progress in simulating two types of ENSO—From CMIP5 to CMIP6. Frontiers in Marine Science, 9, 986780. https://doi.org/10.3389/fmars.2022.986780
- Hu, S. N., Fedorov, A. V., Lengaigne, M., & Guilyardi, E. (2014). The impact of westerly wind bursts on the diversity and predictability of El Niño events: An ocean energetics perspective. *Geophysical Research Letters*, 41(13), 4654–4663. https://doi.org/10.1002/2014g1059573
- Hu, Z. Z., Kumar, A., Xue, Y., & Jha, B. (2014). Why were some La Ninas followed by another La Nina? Climate Dynamics, 42(3-4), 1029-1042. https://doi.org/10.1007/s00382-013-1917-3
- Huang, B., Thorne, P. W., Banzon, V. F., Boyer, T., Chepurin, G., Lawrimore, J. H., et al. (2017). Extended reconstructed sea surface temperature, Version 5 (ERSSTv5): Upgrades, validations, and intercomparisons [Dataset]. *Journal of Climate*, 30(20), 8179–8205. https://doi.org/10.1175/ JCLI-D-16-0836.1
- Jin, F. F. (1997). An equatorial Ocean recharge paradigm for ENSO. Part I: Conceptual model. *Journal of the Atmospheric Sciences*, 54(7), 811–829. https://doi.org/10.1175/1520-0469(1997)054<0811;aeorpf>2.0.co;2
- Kao, H. Y., & Yu, J. Y. (2009). Contrasting eastern-pacific and central-pacific types of ENSO. Journal of Climate, 22(3), 615–632. https://doi.org/10.1175/2008JCLI2309.1
- Kim, S. T., Yu, J. Y., Kumar, A., & Wang, H. (2012). Examination of the two types of ENSO in the NCEP CFS model and its extratropical associations. Monthly Weather Review, 140(6), 1908–1923. https://doi.org/10.1175/Mwr-D-11-00300.1
- Kug, J. S., Choi, J., An, S. I., Jin, F. F., & Wittenberg, A. T. (2010). Warm pool and cold tongue El niño events as simulated by the GFDL 2.1 coupled GCM. *Journal of Climate*, 23(5), 1226–1239. https://doi.org/10.1175/2009jcli3293.1
- Lai, A. W. C., Herzog, M., & Graf, H. F. (2015). Two key parameters for the El Niño continuum: Zonal wind anomalies and Western Pacific subsurface potential temperature. Climate Dynamics, 45(11–12), 3461–3480. https://doi.org/10.1007/s00382-015-2550-0
- Latif, M., Sterl, A., Maierreimer, E., & Junge, M. M. (1993). Climate variability in a coupled GCM.1. the tropical Pacific. *Journal of Climate*, 6(1), 5–21. https://doi.org/10.1175/1520-0442(1993)006<0005:Cviacg>2.0.Co;2
- Leloup, J., Lengaigne, M., & Boulanger, J. P. (2008). Twentieth century ENSO characteristics in the IPCC database. *Climate Dynamics*, 30(2–3),
- 277–291. https://doi.org/10.1007/s00382-007-0284-3
  Li, A. Q., Ji, C. O., & Fang, X. F. (2025). A new Insight on El niño diversity: Decadal variability in westerly wind bursts. *Atmospheric Science*
- Letters, 26(5), e1301. https://doi.org/10.1002/asl.1301
  McPhaden, M. J., Lee, T., & McClurg, D. (2011). El Niño and its relationship to changing background conditions in the tropical Pacific Ocean.
- McPhaden, M. J., Lee, T., & McClurg, D. (2011). El Niño and its relationship to changing background conditions in the tropical Pacific Ocean Geophysical Research Letters, 38(15), L15709. https://doi.org/10.1029/2011g1048275
- Morel, P. G. (2018). Grammar of graphics plotting in Matlab. Journal of Open Source Software, 3(23), 568. https://doi.org/10.21105/joss.00568
  Ronneberger, O., Fischer, P., & Brox, T. (2015). U-Net: Convolutional networks for biomedical image segmentation. In Proceedings of the 18th international conference on medical image computing and computer assisted intervention, Munich, Germany (pp. 234–241). Springer. https://doi.org/10.1007/978-3-319-24574-4\_28
- Stuecker, M. F. (2018). Revisiting the Pacific meridional mode. Scientific Reports UK, 8(1), 3216. https://doi.org/10.1038/s41598-018-21537-0
  Tao, L. J., & Duan, W. S. (2019). Using a nonlinear forcing singular vector approach to reduce model error effects in ENSO forecasting. Weather and Forecasting, 34(5), 1321–1342. https://doi.org/10.1175/Waf-D-19-0050.1
- Tao, L. J., & Duan, W. S. (2022). A novel precursory signal of the Central Pacific El Niño event: Eastern Pacific cooling mode. Climate Dynamics, 59(9–10), 2599–2617. https://doi.org/10.1007/s00382-022-06229-w
- Tao, L. J., Duan, W. S., & Jiang, L. (2022). Model errors of an intermediate model and their effects on realistic predictions of El Niño diversity. International Journal of Climatology, 42(15), 7443–7464. https://doi.org/10.1002/joc.7656
- Tao, L. J., Duan, W. S., & Vannitsem, S. (2020). Improving forecasts of El Niño diversity: A nonlinear forcing singular vector approach. Climate Dynamics, 55(3–4), 739–754. https://doi.org/10.1007/s00382-020-05292-5
- Timmermann, A., An, S. I., Kug, J. S., Jin, F. F., Cai, W., Capotondi, A., et al. (2018). El Niño-Southern Oscillation complexity. *Nature*, 559(7715), 535–545. https://doi.org/10.1038/s41586-018-0252-6
- Tokarska, K. B., Stolpe, M. B., Sippel, S., Fischer, E. M., Smith, C. J., Lehner, F., & Knutti, R. (2020). Past warming trend constrains future warming in CMIP6 models. *Science Advances*, 6(12), eaaz9549. https://doi.org/10.1126/sciadv.aaz9549
- Vialard, J., Jin, F., McPhaden, M. J., Fedorov, A., Cai, W., An, S., et al. (2025). The El Niño Southern Oscillation (ENSO) recharge oscillator conceptual model: Achievements and future prospects. *Reviews of Geophysics*, 63(1), e2024RG000843. https://doi.org/10.1029/2024RG000843
- Vimont, D. J., Alexander, M. A., & Newman, M. (2014). Optimal growth of Central and East Pacific ENSO events. *Geophysical Research Letters*, 41(11), 4027–4034. https://doi.org/10.1002/2014g1059997
- Xu, K., Huang, R. X., Wang, W. Q., Zhu, C. W., & Lu, R. Y. (2017). Thermocline fluctuations in the equatorial Pacific related to the two types of El Niño events. *Journal of Climate*, 30(17), 6611–6627. https://doi.org/10.1175/Jcli-D-16-0291.1
- Yang, W. S., Liu, C. Y., Köhl, A., Wang, J., Wang, X., & Wang, F. (2023). The adjoint-based favorable winds for the generation of the central Pacific El Niño. *Journal of Climate*, 36(16), 5491–5510. https://doi.org/10.1175/Jcli-D-22-0548.1
- Yu, J. Y., & Fang, S. W. (2018). The distinct contributions of the seasonal footprinting and charged-discharged mechanisms to ENSO complexity. Geophysical Research Letters, 45(13), 6611–6618. https://doi.org/10.1029/2018gl077664
- Yu, J. Y., & Kim, S. T. (2010). Identification of Central-Pacific and Eastern-Pacific types of ENSO in CMIP3 models. Geophysical Research Letters, 37(15). https://doi.org/10.1029/2010gl044082
- Zebiak, S. E., & Cane, M. A. (1987). A model El-Niño Southern oscillation. *Monthly Weather Review*, 115(10), 2262–2278. https://doi.org/10.1175/1520-0493(1987)115<2262:Ameno>2.0.Co;2
- Zhang, R. H., Busalacchi, A. J., & Dewitt, D. G. (2008). The roles of atmospheric Stochastic Forcing (SF) and Oceanic entrainment temperature (Te) in decadal modulation of ENSO. *Journal of Climate*, 21(4), 674–704. https://doi.org/10.1175/2007jcli1665.1
- Zhang, R. H., & Gao, C. (2016). The IOCAS intermediate coupled model (IOCAS ICM) and its real-time predictions of the 2015–2016 El Niño event. Scientific Bulletin, 61(13), 1061–1070. https://doi.org/10.1007/s11434-016-1064-4

TAO AND DUAN 19 of 20



### Journal of Geophysical Research: Oceans

10.1029/2025JC022777

- Zhang, R. H., Zebiak, S. E., Kleeman, R., & Keenlyside, N. (2003). A new intermediate coupled model for El Niño simulation and prediction. *Geophysical Research Letters*, 30(19), 20–21. https://doi.org/10.1029/2003g1018010
- Zheng, Y. C., Duan, W. S., Tao, L. J., & Ma, J. J. (2023). Using an ensemble nonlinear forcing singular vector data assimilation approach to address the ENSO forecast uncertainties caused by the "spring predictability barrier"s and El Niño diversity. *Climate Dynamics*, 61(11–12), 4971–4989. https://doi.org/10.1007/s00382-023-06834-3
- Zhi, X. F., Yang, H., Xu, S. W., Wang, X. C., & Pan, M. T. (2019). A comparative analysis of atmospheric and Oceanic conditions before the occurrence of two types of El Niño events. *Journal of Tropical Meteorology*, 25(1), 34–44. https://doi.org/10.16555/j.1006-8775.2019.01.004

TAO AND DUAN 20 of 20